

RESEARCH ARTICLE

The AKT1-FOXO4 axis reciprocally regulates hemochorial placentation

Keisuke Kozai^{1,¶,*}, Ayelen Moreno-Irusta^{1,¶,**,†}, Khurshheed Iqbal¹, Mae-Lan Winchester^{2,‡}, Regan L. Scott¹, Mikaela E. Simon¹, Masanaga Muto^{1,§}, Marc R. Parrish² and Michael J. Soares^{1,2,3,**}

ABSTRACT

Hemochorial placentation involves the differentiation of invasive trophoblast cells, specialized cells that possess the capacity to exit the placenta and invade into the uterus where they restructure the vasculature. Invasive trophoblast cells arise from a well-defined compartment within the placenta, referred to as the junctional zone in rat and the extravillous trophoblast cell column in human. In this study, we investigated roles for AKT1, a serine/threonine kinase, in placental development using a genome-edited/loss-of-function rat model. Disruption of AKT1 resulted in placental, fetal and postnatal growth restriction. Forkhead box O4 (*Foxo4*), which encodes a transcription factor and known AKT substrate, was abundantly expressed in the junctional zone and in invasive trophoblast cells of the rat placentation site. *Foxo4* gene disruption using genome editing resulted in placentomegaly, including an enlarged junctional zone. AKT1 and FOXO4 regulate the expression of many of the same transcripts expressed by trophoblast cells, but in opposite directions. In summary, we have identified AKT1 and FOXO4 as part of a regulatory network that reciprocally controls critical indices of hemochorial placenta development.

KEY WORDS: AKT1, FOXO4, Trophoblast, Placenta, Pregnancy, Rat, Genome editing

INTRODUCTION

The placenta is an extra-embryonic structure essential for normal fetal development (Maltepe and Fisher, 2015; Burton et al., 2016). Placentas have two main functions: (1) transformation of the maternal environment to support viviparity and (2) regulation of the transfer of nutrients to the fetus (Soares et al., 2018; Knöfler et al., 2019). These specialized functions are ascribed to trophoblast cells, which differentiate along a multi-lineage pathway and are situated within

specific compartments of the placenta (Gardner and Beddington, 1988; Soares et al., 2018; Knöfler et al., 2019; Aplin and Jones, 2021). Placentas of different species vary with respect to shape, size and connectivity to the mother (Wooding and Burton, 2008; Roberts et al., 2016). Placentation in some mammalian species is characterized by trophoblast cells migrating into the maternal uterus where they modify the vasculature facilitating maternal nutrient flow to the placenta (Pijnenborg et al., 1981; Soares et al., 2018). This type of placenta is referred to as hemochorial (Wooding and Burton, 2008; Roberts et al., 2012). In human and rat, hemochorial placentation occurs whereby invasive trophoblast cells migrate deep into the uterine parenchyma (Pijnenborg et al., 1981; Soares et al., 2012). Regulation of deep hemochorial placentation is poorly understood. The rat represents a useful animal model for investigating the regulation of deep hemochorial placentation (Pijnenborg and Vercruyse, 2010; Soares et al., 2012; Shukla and Soares, 2022).


The rat placenta can be divided into two main compartments: the junctional zone and the labyrinth zone (Soares et al., 2012). The junctional zone compartment of the placenta is situated proximal to the uterine endometrium and is responsible for transforming the maternal environment, whereas the labyrinth zone is located between the junctional zone and fetus where it facilitates nutrient delivery to the fetus (Knipp et al., 1999; Soares et al., 2012). Junctional zone-specific functions include the production of peptide and steroid hormones that target maternal organs and the generation of invasive trophoblast cells that migrate into and restructure the uterine parenchyma (Soares et al., 1996; 2012). The extravillous trophoblast cell column is a structure within the human placentation site, which shares some of these same responsibilities (Soares et al., 2018; Knöfler et al., 2019). The junctional zone and extravillous trophoblast cell column are pivotal to the regulation of maternal adaptations to pregnancy, yet little is known about how they are regulated.

Here, we focus on the phosphatidylinositol 3-kinase (PI3K)/AKT pathway and its involvement in regulation of junctional zone biology. AKT1 is one of three AKT serine/threonine kinases and represents an integral component of signal transduction pathways regulating cell proliferation, differentiation, migration, survival and metabolism (Manning and Toker, 2017; Cole et al., 2019). AKT1 has also been implicated in placentation and trophoblast cell development through rodent mutagenesis experiments and investigations with human trophoblast cells (Kamei et al., 2002; Yang et al., 2003; Qiu et al., 2004; Dash et al., 2005; Kent et al., 2010; 2011, 2012; Plaks et al., 2011; Haslinger et al., 2013; Sharma et al., 2016). Disruptions in AKT signaling have been connected to trophoblast cell dysfunction leading to recurrent pregnancy loss, pre-eclampsia and infertility (Pollheimer and Knöfler, 2005; Ferretti et al., 2007; Fisher, 2015; Burton and Jauniaux, 2018). Here, we show that AKT1 inactivation leads to placental and fetal growth restriction in the rat. AKT1 acts via phosphorylation of its target proteins leading to functional changes,

¹Institute for Reproductive and Developmental Sciences, Department of Pathology & Laboratory Medicine, University of Kansas Medical Center, Kansas City, KS 66160, USA. ²Department of Obstetrics and Gynecology, University of Kansas Medical Center, Kansas City, KS 66160, USA. ³Center for Perinatal Research, Children's Mercy Research Institute, Children's Mercy, Kansas City, MO 64108, USA.

*Present address: Department of Obstetrics and Gynecology, University of Missouri-Kansas City School of Medicine, Kansas City, MO 64108, USA. †Present address: Department of Obstetrics and Gynecology, University Hospital, Case Western Reserve University, Beachwood, OH 44122, USA. ‡Present address: Department of Stem Cells and Human Disease Models, Research Center for Animal Life Science, Shiga University of Medical Science, Seta, Tsukinowa-cho, Otsu, Shiga 520-2192, Japan. §These authors contributed equally to this work

**Authors for correspondence (amoreno2@kumc.edu; msoares@kumc.edu)

 K.K., 0000-0003-2645-7431; A.M., 0000-0001-6810-6475; R.L.S., 0000-0001-6294-5294; M.E.S., 0000-0001-5301-2724; M.J.S., 0000-0001-7158-1592

Handling Editor: Liz Robertson

Received 1 July 2022; Accepted 21 December 2022

including activation or inhibition of target protein function (Manning and Toker, 2017; Cole et al., 2019). We have identified forkhead box O4 (FOXO4), a transcription factor, as an AKT1 substrate within the rat junctional zone and in rat trophoblast cells and demonstrated FOXO4 involvement in junctional zone development and the regulation of trophoblast cell differentiation.

RESULTS

Generation of an *Akt1* mutant rat model

AKT1 and phosphorylated AKT are ubiquitously expressed throughout the rat placentation site (Fig. S1A). We examined the role of AKT1 in regulating deep placentation in the rat using CRISPR/Cas9 genome editing. A mutant rat strain possessing a 1332 bp deletion within the *Akt1* gene was generated (Fig. 1A,B). The deletion included part of exon 4, the entire region spanning exons 5 and 6, and part of exon 7 and led to a frameshift and premature stop codon (Fig. 1A,B). The deletion effectively removed the kinase domain and regulatory regions of AKT1 (Fig. 1C). The *Akt1* mutation was successfully transmitted through the germline. A rat colony possessing the *Akt1* mutation was established and maintained via heterozygous×heterozygous breeding. Mating of heterozygotes produced the predicted Mendelian ratio (Fig. 1D; Table S1). Placental tissues possessing a homozygous deletion within the *Akt1* locus (*Akt1*^{-/-}) were deficient in AKT1 protein and exhibited prominent deficits in pan-AKT and phospho-AKT protein expression (Fig. 1E). Residual AKT activity could have arisen from AKT2 or AKT3, as previously demonstrated for rat trophoblast cells (Kent et al., 2011). These findings support the successful disruption

of the *Akt1* locus and are consistent with AKT1 being the predominant AKT isoform within the placenta (Yang et al., 2003; Kent et al., 2011; Haslinger et al., 2013).

AKT1 deficiency results in placental, fetal and postnatal growth restriction

Disruption of the *Akt1* locus in the mouse affects placental, fetal and postnatal growth (Chen et al., 2001; Cho et al., 2001; Yang et al., 2003; Plaks et al., 2011; Kent et al., 2012). We observed a similar phenotype in the rat. Gestation day (gd) 18.5 placental and fetal weights and postnatal pup weights were significantly smaller in the *Akt1*^{-/-} rat model compared with *Akt1*^{+/+} rats (Fig. 2A-H). Junctional and labyrinth zone compartments of the placenta were also significantly smaller in *Akt1*^{-/-} placentas (Fig. 2D,E,I).

AKT1 regulates junctional zone and invasive trophoblast cell phenotypes

Transcript profiles were determined for *Akt1*^{+/+} and *Akt1*^{-/-} gd 18.5 junctional zone tissues using RNA-sequencing (RNA-seq). The size and morphological phenotypes associated with inactivation of AKT1 were associated with distinct transcript profiles (Fig. 3; Table S2). Disruption of AKT1 resulted in upregulation of 254 transcripts and downregulation of 333 transcripts (Table S2). Pathway analysis included signatures for cell cycle, DNA replication, cellular senescence, and PI3K-AKT signaling pathways (Fig. 3A; Table S3). Transcripts encoding cell cycle progression were consistently repressed in the *Akt1*^{-/-} junctional zones (Fig. 3A,B). In addition, we also observed prominent downregulation of a member of the

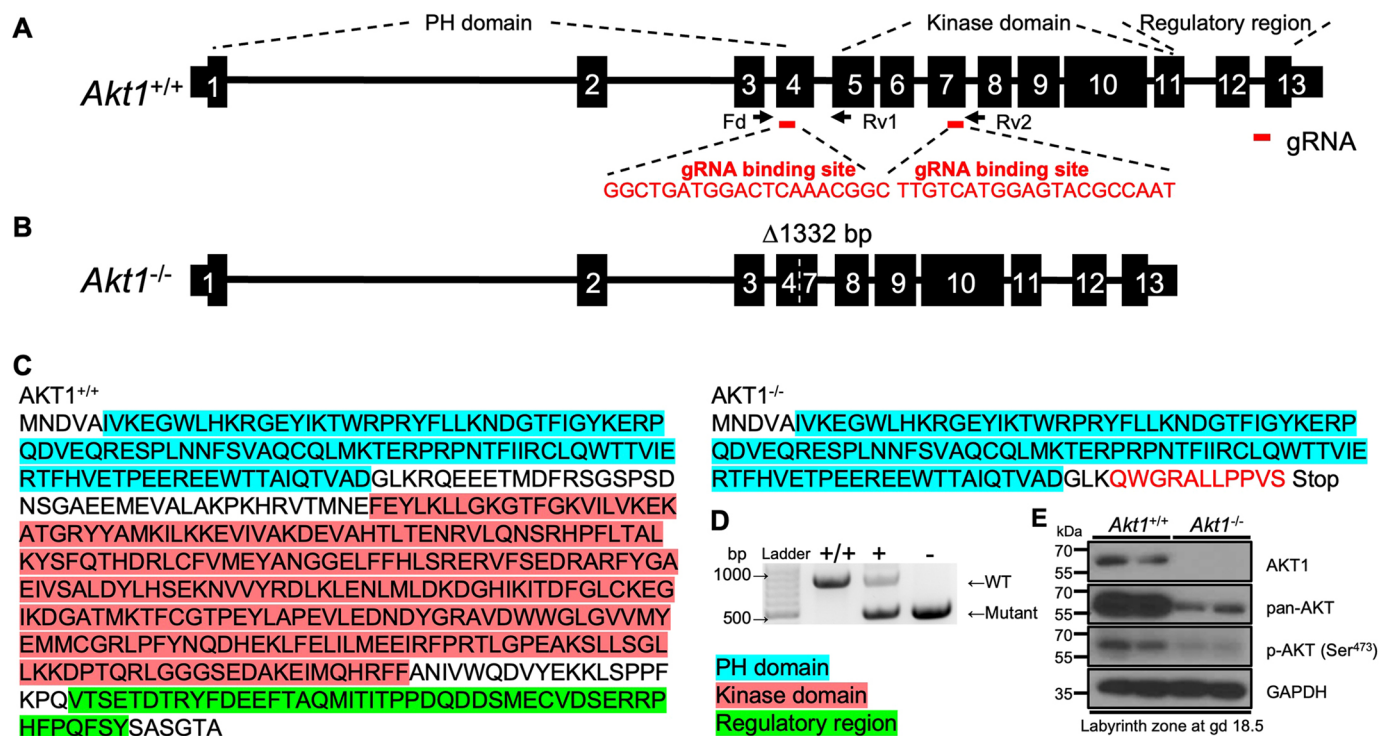


Fig. 1. *In vivo* genome editing of the rat *Akt1* locus. (A) Schematic of the rat *Akt1* gene (*Akt1*^{+/+}) and guide RNA target sites within exons 4 and 7 (NM_033230.3). Black boxes represent exons, and red bars beneath exons 4 and 7 correspond to the 5' and 3' guide RNAs used in the genome editing. (B) The mutant *Akt1* allele (*Akt1*^{-/-}) possesses a 1332 bp deletion. Parts of exons 4 and 7 and all of exons 5 and 6 were deleted, leading to a frameshift and premature stop codon in exon 7. (C) Amino acid sequences for AKT1^{+/+} and AKT1^{-/-}. The red sequence corresponds to the frameshift in exon 7. The blue, red and green highlighted amino acid sequence regions correspond to the pleckstrin homology (PH), kinase, and regulatory domains, respectively. (D) Offspring were backcrossed to wild-type rats, and heterozygous mutant rats were intercrossed to generate homozygous mutants. Wild-type (+/+; WT), heterozygous (+/-) and homozygous mutant (-/-) genotypes were detected by PCR. (E) Western blot analysis of AKT1, pan-AKT and phospho (p)-AKT (Ser⁴⁷³) protein in *Akt1*^{+/+} and *Akt1*^{-/-} placentas at gd 18.5. GAPDH was used as a loading control.

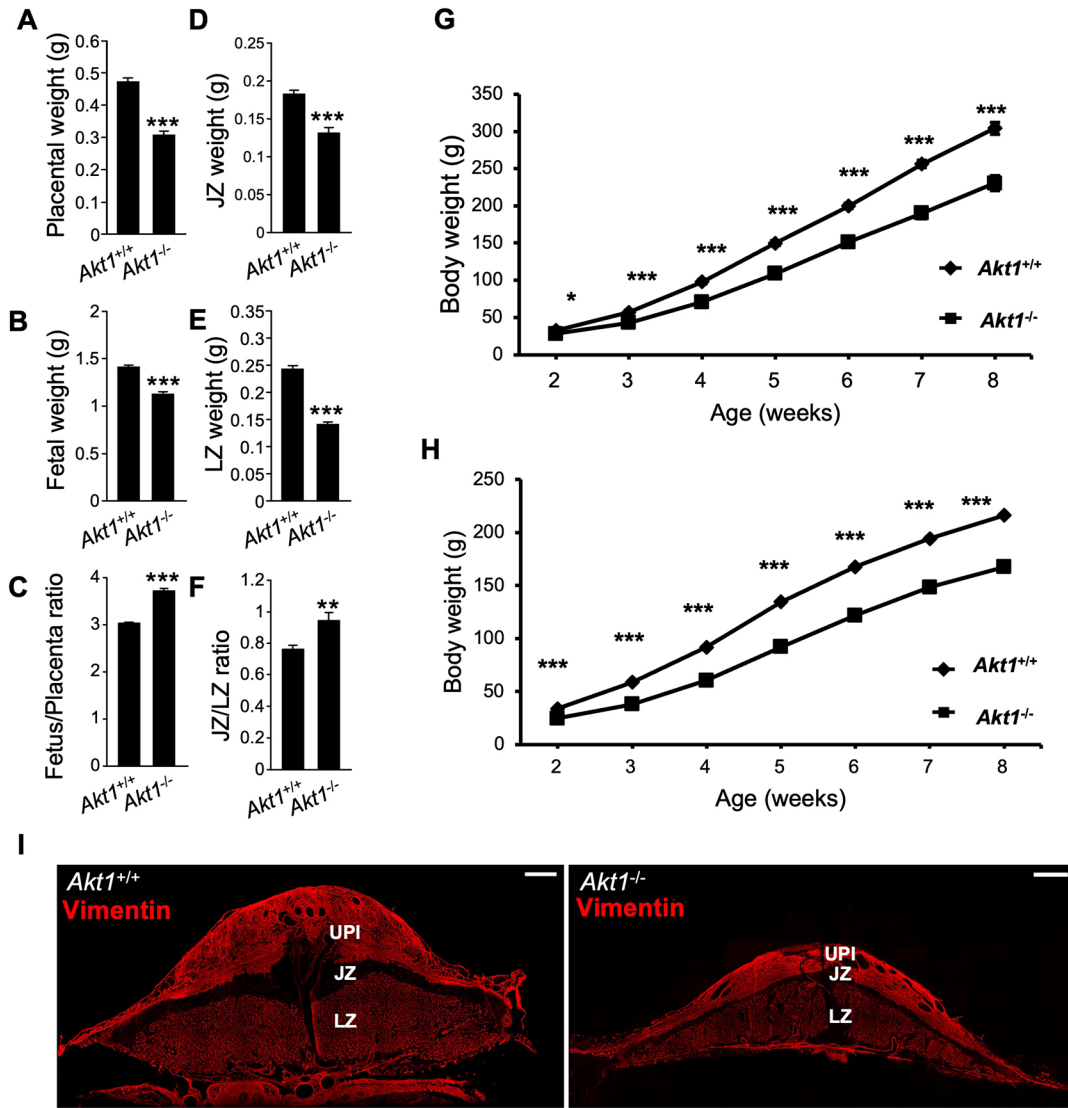


Fig. 2. *Akt1*^{-/-} placentas and fetuses are growth restricted, and *Akt1*^{-/-} rats exhibit postnatal growth restriction. (A-C) Placentas (A) and fetuses (B) were dissected from *Akt1*^{+/+} intercrosses at gd 18.5 and weighed; the fetus/placenta ratio is shown in C. (D-F) Placentas were then separated into junctional zone (JZ; D) and labyrinthine zone (LZ; E) compartments and weighed; the JZ/LZ ratio is shown in F. Graphs represent mean±s.e.m. *Akt1*^{+/+}, n=22 from 6 dams; *Akt1*^{-/-}, n=17 from 6 dams. Asterisks denote statistical differences (***P*<0.01; ****P*<0.001) as determined by unpaired, two-tailed Student's (*A-E*) or Welch's (*F*) *t*-test. (G,H) Body weights of male (G) and female (H) *Akt1*^{+/+} and *Akt1*^{-/-} pups were measured from two to eight weeks after birth. Graphs represent mean±s.e.m. n=13-23/group. Asterisks denote statistical differences (**P*<0.05; ****P*<0.001) as determined by unpaired, two-tailed Student's *t*-test. (I) Vimentin immunostaining of gd 18.5 *Akt1*^{+/+} and *Akt1*^{-/-} placentation sites. The JZ is negative for vimentin immunostaining, whereas the uterine-placental interface (UPI) and LZ stain positive for vimentin. Images are representative of five samples. Scale bars: 1000 μm.

expanded prolactin (PRL) gene family, *Prl8a4* (2-fold), and the upregulation of cellular communication network factor 3 (3-fold), *Ccn3* (also called *Nov*; Fig. 3B).

The junctional zone serves as the source of invasive trophoblast cells entering the uterus. Consequently, we investigated the uterine-placental interface of *Akt1*^{+/+} and *Akt1*^{-/-} placentas and monitored the surface area occupied by intrauterine invasive trophoblast cells and the expression of invasive trophoblast cell-specific transcripts. *Akt1*^{-/-} invasive trophoblast cells exhibited decreased infiltration into the uterus (Fig. 3C-E). The decrease in trophoblast invasion was proportional to the size of *Akt1*^{+/+} versus *Akt1*^{-/-} junctional zone compartments (Fig. S1B). We also observed an approximately 50% decrease in the expression of cytochrome transcripts, which are expressed by invasive trophoblast cells within the uterine-placental interface (Fig. 3F).

Collectively, the data indicate that AKT1 signaling has profound effects on development of the junctional zone and the invasive trophoblast cell lineage.

FOXO4 is a target of PI3K/AKT signaling

Forkhead box (FOX) transcription factors are known targets of PI3K/AKT signaling and have key roles in regulating developmental processes (Lam et al., 2013; Schmitt-Ney, 2020; Herman et al., 2021). We interrogated RNA-seq datasets from the wild-type gd 18.5 junctional zone for FOX family transcription factors. Transcripts for several FOX transcription factors were detected [transcripts per million (TPM) value ≥1.0] (Fig. 4A). *Foxo4* transcripts were striking in their abundance relative to all other FOX family members. AKT1 did not significantly affect expression levels for any of the FOX family transcripts (Table S2). *Foxo4* transcripts were specifically

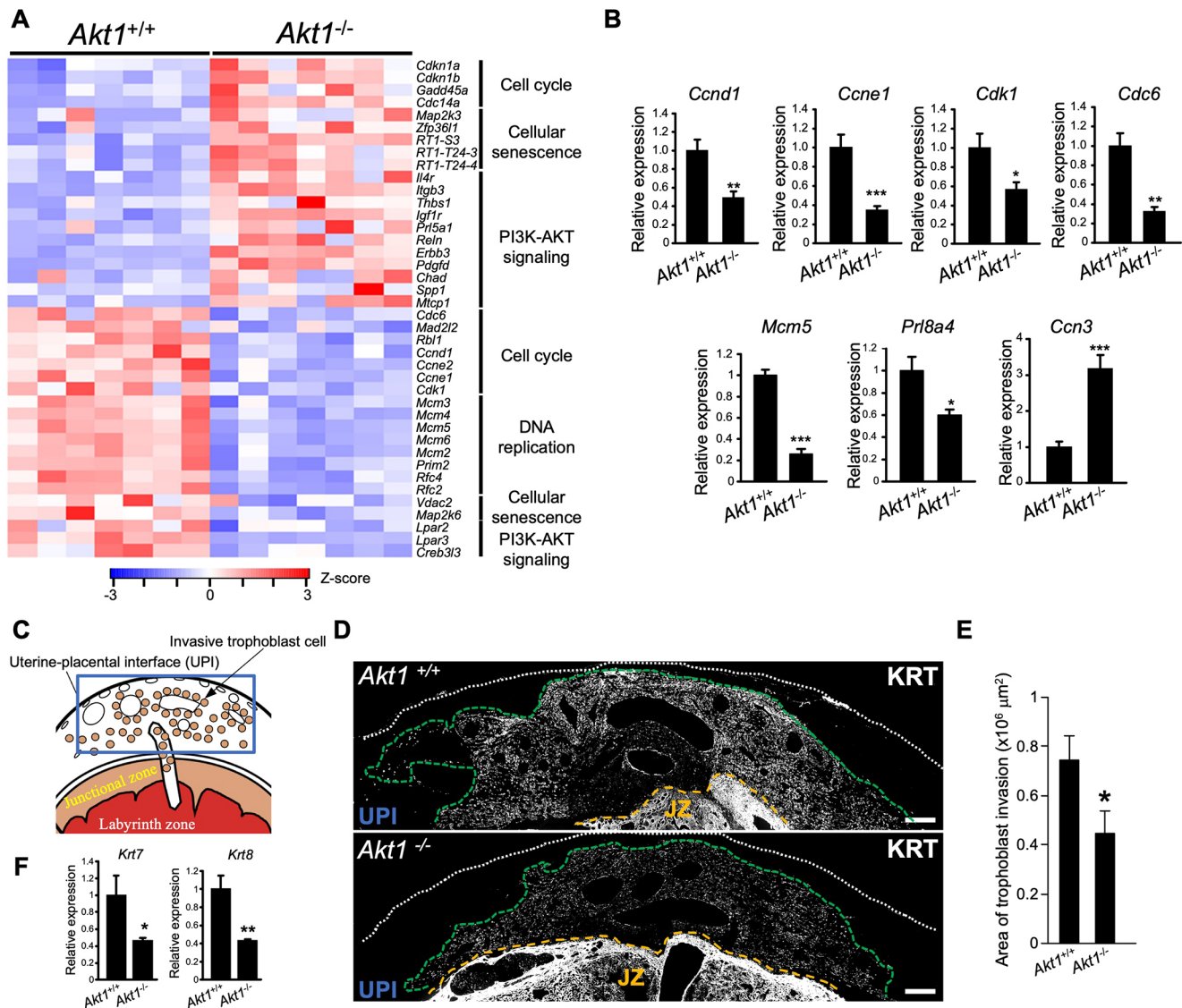


Fig. 3. AKT1 regulates junctional zone and invasive trophoblast cell phenotypes. (A) Heat maps depicting differentially expressed genes between *Akt1*^{+/+} and *Akt1*^{-/-} junctional zones. The heatmap color keys represent z-scores of TPM values. (B) RT-qPCR validation of RNA-seq results ($n=6$ /group). Graphs represent mean \pm s.e.m. Asterisks denote statistical difference (* $P<0.05$; ** $P<0.01$; *** $P<0.001$) as determined by unpaired, two-tailed Student's (*Ccnd1*, *Ccne1*, *Cdk1*, *Mcm5*, *Prl8a4* and *Ccn3*) or Welch's (*Cdc6*) *t*-test. (C) Schematic of a late gestation placental site. The uterine-placental interface (UPI), the site for intrauterine trophoblast invasion, is highlighted in the boxed area. (D) AKT1 deficiency affected intrauterine trophoblast cell invasion. Trophoblast cells were immunostained for pan-cytokeratin (KRT). Representative images are shown. The extent of intrauterine trophoblast invasion is demarcated using a green dashed line. The white dotted line represents the outer border of the uterus, and the yellow dashed line represents the uterine border with the placenta. JZ, junctional zone. Images are representative of five samples. Scale bars: 500 μ m. (E) The area of intrauterine trophoblast invasion is graphically depicted ($n=6$ /group). Graphs represent mean \pm s.e.m. An asterisk denotes statistical difference (* $P<0.05$) as determined by unpaired, two-tailed Student's *t*-test. (F) RT-qPCR measurements of *Krt7* and *Krt8* transcripts, signature markers for invasive trophoblast cells, within dissected uterine-placental interface tissue specimens at gd 18.5 (*Akt1*^{+/+}, $n=21$; *Akt1*^{-/-}, $n=16$). Graphs represent mean \pm s.e.m. Asterisks denote statistical difference (* $P<0.05$; ** $P<0.01$; *** $P<0.001$) as determined by unpaired, two-tailed Welch's *t*-test.

localized to the junctional zone and a subset of invasive trophoblast cells (Fig. 4B,C). FOXO4 protein and phosphorylated FOXO4 exhibited similar tissue distributions (Fig. S2A). Phosphorylated FOXO4 protein was significantly diminished in *Akt1* null junctional zones (Fig. 4D; Fig. S2B). We next explored FOXO4 in differentiated rat trophoblast stem cells (TSCs) (Asanoma et al., 2011). Rat TSCs can differentiate into trophoblast giant cells and spongiotrophoblast cells and represent an effective *in vitro* model for investigating junctional zone development (Chakraborty et al., 2011, 2016; Asanoma et al., 2012; Kubota et al., 2015; Muto et al., 2021; Varberg et al., 2021). *Foxo4* transcript and total and phosphorylated

FOXO4 protein showed striking increases in abundance following TSC differentiation (Fig. 4E,F). As previously demonstrated, AKT activity increased following trophoblast cell differentiation (Kamei et al., 2002; Kent et al., 2010, 2011; Fig. 4G). AKT activation was required for optimal FOXO4 phosphorylation (Fig. 4G). Intracellular distributions of FOXO4 and phosphorylated FOXO4 were affected by inhibition of PI3K in differentiated rat TSCs (Fig. 4H). Disruption of PI3K/AKT signaling shifted FOXO4 and phosphorylated FOXO4 to the nucleus (Fig. 4H). Inhibition of PI3K in rat TSCs did not significantly impact a measure of apoptosis (cleaved caspase 3) but did reveal evidence for increased autophagy

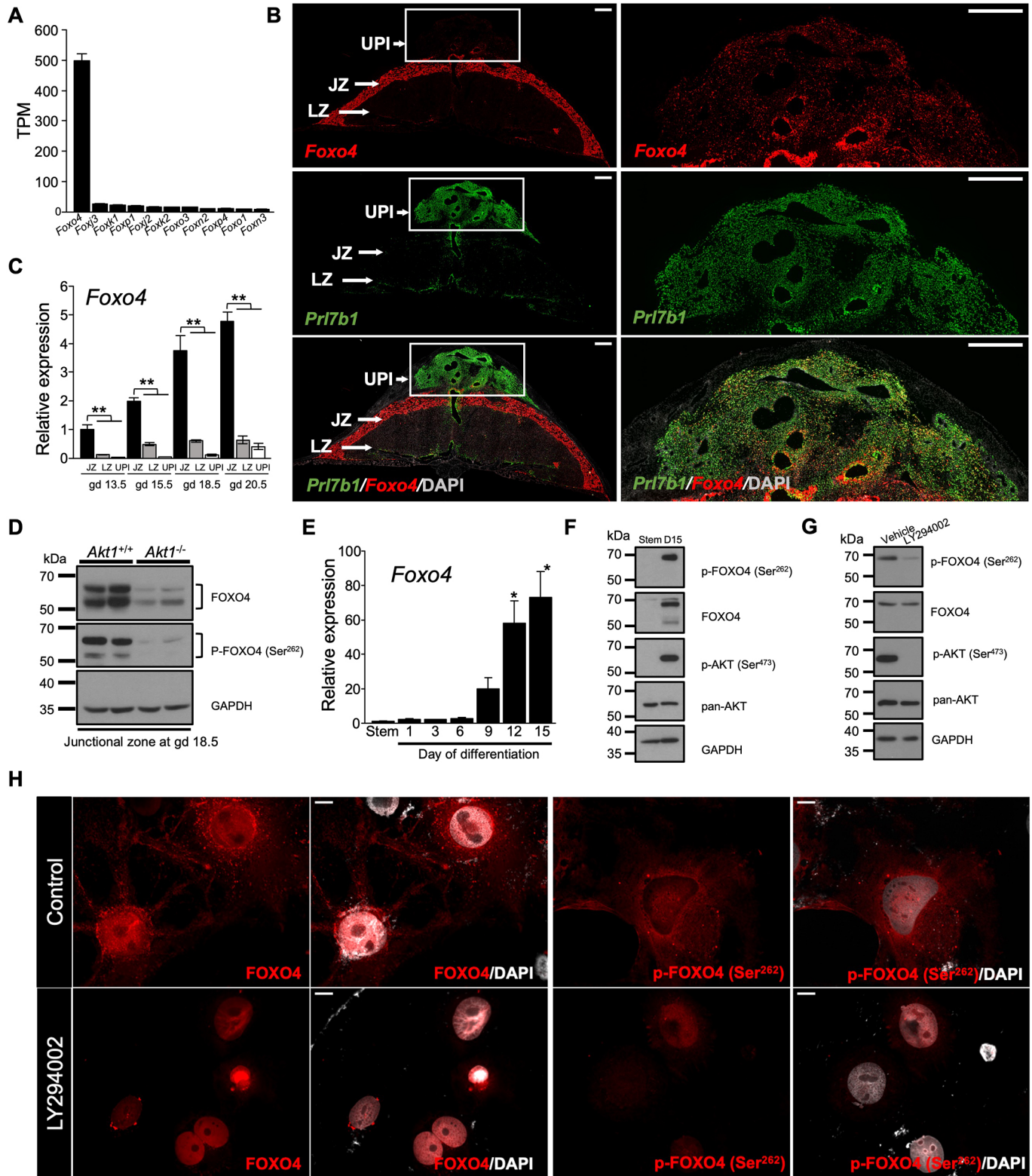


Fig. 4. See next page for legend.

(Fig. S2C,D). Thus, we provide support for a link between PI3K/ AKT signaling and FOXO4 in trophoblast cell lineage development.

Generation of a Foxo4 mutant rat model

We examined the role of FOXO4 in regulating placentation in the rat using CRISPR/Cas9 genome editing. The Foxo4 gene consists of

four exons and resides on the X chromosome (Liu et al., 2020). A mutant rat strain possessing a 3096 bp deletion within the Foxo4 gene was generated (Fig. 5A,B). The deletion included the 3' part of exon 2 and the 5' part of exon 3 and led to a frameshift and a premature stop codon (Fig. 5A,B). The deletion effectively disrupted the conserved forkhead DNA-binding domain and

Fig. 4. FOXO4 is a target of PI3K/AKT signaling. (A) Expression of transcripts for several FOX transcription factors in the junctional zone. (B) *In situ* localization of transcripts for *Foxo4* with *Pr17b1* (invasive trophoblast-specific transcript) in the placentation site at gd 18.5 of rat pregnancy. Boxed areas are shown at higher magnification on the right. Scale bars: 1000 μ m. (C) RT-qPCR measurements of *Foxo4* transcripts in the uterine-placental interface, junctional and labyrinth zones during the second half of gestation ($n=6-9$ /group). Graphs represent mean \pm s.e.m. Asterisks denote statistical difference (** $P<0.01$) as determined by Steel test. (D) Western blot analysis of phospho (P)-FOXO4 (Ser²⁶²) and FOXO4 proteins in *Akt1*^{+/+} and *Akt1*^{-/-} placentas at gd 18.5. GAPDH was used as a loading control. (E) RT-qPCR measurements of *Foxo4* transcripts in the stem state and following induction of differentiation ($n=4-6$ /group). Graphs represent mean \pm s.e.m. Asterisks denote statistical difference (versus 'Stem'; * $P<0.05$) as determined by Dunnett's test. (F,G) Western blot analysis of phospho (p)-FOXO4 (Ser²⁶²), FOXO4, p-AKT (Ser⁴⁷³) and pan-AKT proteins in the stem and differentiating (day 15 of differentiation, D15) states (F), and in the differentiating state (D15) following treatment with vehicle (0.1% DMSO) or a PI3K inhibitor (LY294002, 10 μ M) for 1 h (G). GAPDH was used as a loading control. (H) Rat TSCs following 15 days in differentiating conditions were treated with vehicle (0.1% DMSO, Control) or a PI3K inhibitor (LY294002, 10 μ M) for 24 h and then immunostained for phospho (p)-FOXO4 (Ser²⁶²) and FOXO4. Representative images are shown. Scale bars: 50 μ m. JZ, junctional zone; LZ, labyrinth zone; UPI, uterine-placental interface. Images are representative of five samples.

removed nuclear localization, nuclear export, and transactivation domains of FOXO4 (Fig. 5C). The *Foxo4* mutation was successfully transmitted through the germline (Fig. 5D; Table S4). A rat colony possessing the *Foxo4* mutation was

established and maintained via hemizygous male \times wild-type female breeding, which produced the predicted Mendelian ratio (Table S4). Junctional zone tissues possessing a maternally inherited *Foxo4* mutation (*Foxo4*^{X^m-}) were deficient in FOXO4 protein (Fig. 5E). The results are consistent with paternal silencing of X chromosome-linked genes expressed in extra-embryonic tissues (Takagi and Sasaki, 1975; West et al., 1978; Hemberger, 2002). FOXO4 was successfully disrupted in the rat.

FOXO4 deficiency results in placentomegaly and a modified junctional zone phenotype

Placentation site phenotypes of mice possessing mutations at the *Foxo4* locus have not been described (Hosaka et al., 2004). Rats possessing a maternally inherited mutant *Foxo4* allele (*Foxo4*^{X^m-}) exhibited placentomegaly and decreased placental efficiency (fetal/placental weight ratio) when examined on gd 18.5 (Fig. 6A-C) and gd 20.5 (Fig. S3A-C). In contrast, a paternally inherited mutant *Foxo4* allele did not significantly affect placental or fetal weights (Fig. S3D,E). FOXO4 deficiency-associated placentomegaly included significantly larger junctional and labyrinth zones (Fig. 6D-G; Fig. S3F-H), but did not affect the intrauterine invasive trophoblast cell lineage (Fig. S4). Transcript profiles were determined for wild-type (*Foxo4*^{X^m+}) and *Foxo4*^{X^m-} gd 18.5 junctional zone tissues by RNA-seq (Fig. 6H). Disruption of FOXO4 resulted in upregulation of 369 transcripts and downregulation of 845 transcripts (Table S5). Pathway analysis included signatures for PI3K-AKT signaling, cell cycle, DNA

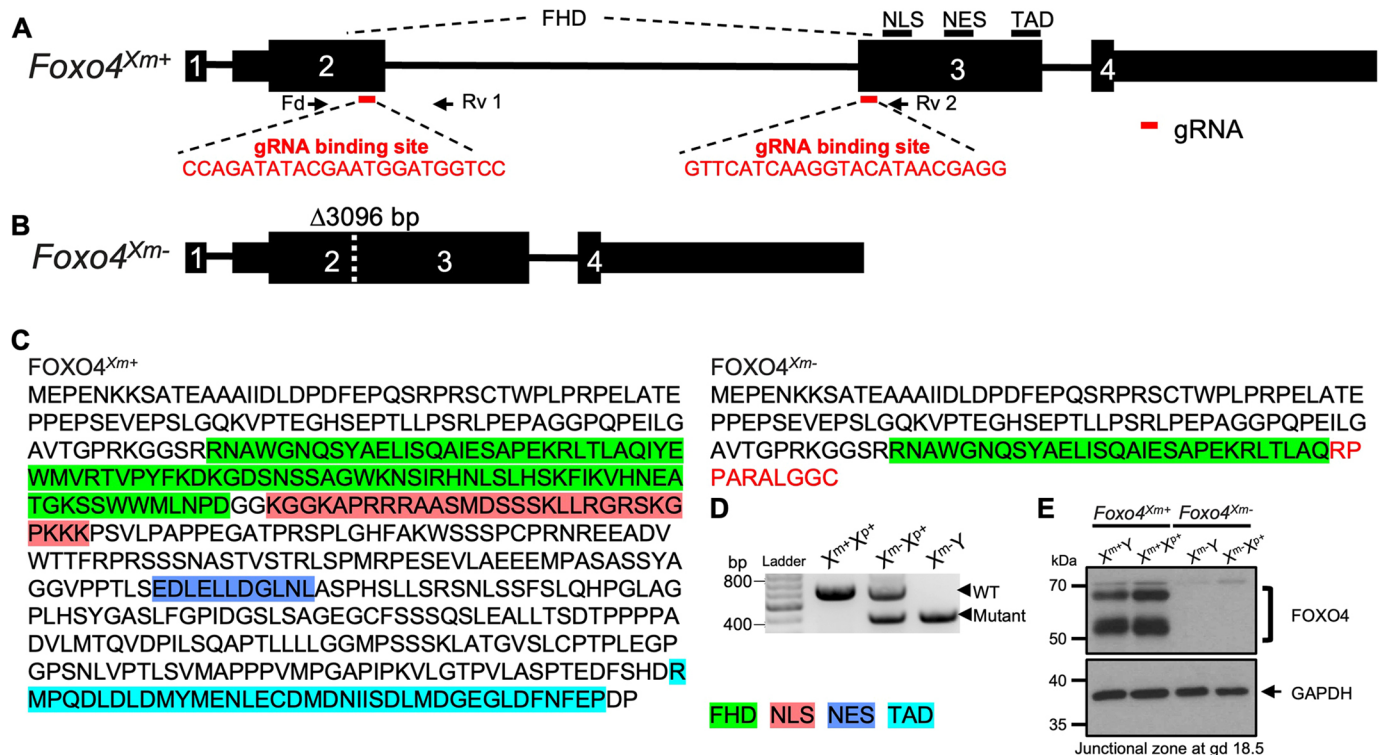


Fig. 5. *In vivo* genome editing of the rat *Foxo4* locus. (A) Schematic of the rat *Foxo4* gene (*Foxo4*^{X^m+}) and guide RNA target sites within exons 2 and 3 (NM_001106943.1). Black boxes represent exons, and red bars beneath exons 2 and 3 correspond to the 5' and 3' guide RNAs used in the genome editing. (B) The mutant *Foxo4* allele (*Foxo4*^{X^m-}) possesses a 3096 bp deletion. Parts of exons 2 and 3 are deleted, leading to a frameshift and premature stop codon in exon 3. (C) Amino acid sequences for FOXO4^{X^m+} and FOXO4^{X^m-}. The red sequence corresponds to the frameshift in exon 3. The green, red, dark blue and light blue highlighted amino acid sequence regions correspond to the forkhead winged-helix DNA-binding domain (FHD), nuclear localization sequence (NLS), nuclear export sequence (NES) and transactivation domain (TAD), respectively. (D) Heterozygous mutant female rats were crossed to wild-type male rats to generate hemizygous null male rats. Wild-type (+/+; WT), heterozygous (+/-) and hemizygous null (-/-) genotypes were detected by PCR. (E) Western blot analysis of FOXO4 protein in the junctional zone of *Foxo4*^{X^m+} (X^m+Y and X^m+X^p+) and *Foxo4*^{X^m-} (X^m-Y and X^m-X^p+) placentas at gd 18.5. GAPDH was used as a loading control.

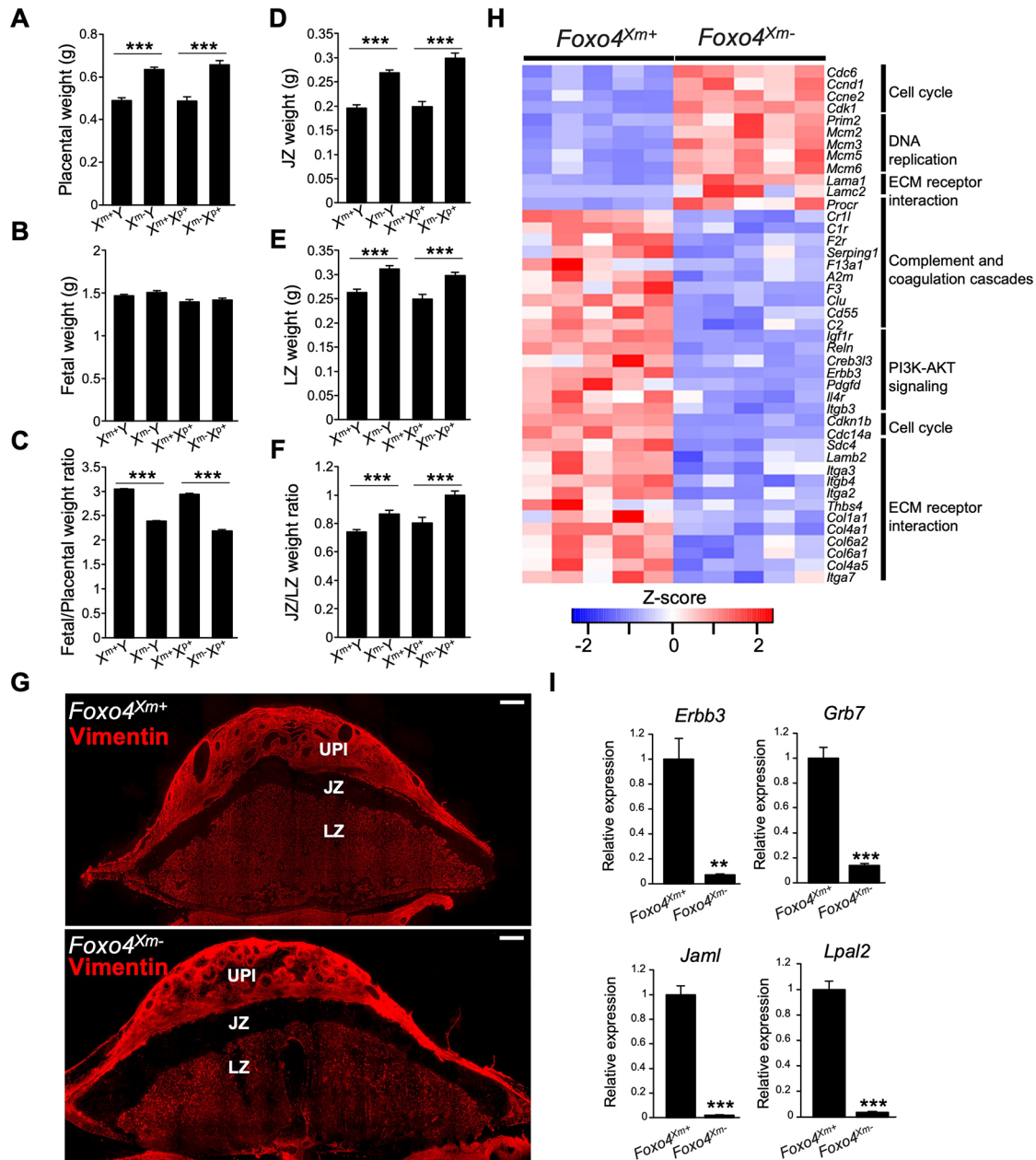


Fig. 6. *Foxo4* hemizygous null and *Foxo4* maternally inherited heterozygous conceptuses exhibit placental overgrowth, and FOXO4 deficiency alters the transcriptomes of the junctional zone. (A-C) Placentas (A) and fetuses (B) were dissected from *Foxo4* heterozygous females mated with wild-type males at gd 18.5 and weighed; the fetus/placenta ratio is shown in C. (D-F) Placentas were then separated into junctional zone (JZ; D) and labyrinth zone (LZ; E) compartments and weighed; the JZ/LZ weight ratio is shown in F. Graphs represent mean \pm s.e.m. $X^{m+}Y$, $n=25$; $X^{m-}Y$, $n=31$; $X^{m+}X^{p+}$, $n=14$; $X^{m-}X^{p+}$, $n=22$ from 8 dams. Asterisks denote statistical differences (***) $P<0.001$ as determined by unpaired, two-tailed Student's *t*-test. (G) Vimentin immunostaining of gd 18.5 *Foxo4*^{*X*^{m+}} and *Foxo4*^{*X*^{m-}} placentation sites. The junctional zone (JZ) is negative for vimentin immunostaining, whereas the uterine-placental interface (UPI) and labyrinth zone (LZ) stain positive for vimentin. Images are representative of five samples. Scale bars: 1000 μ m. (H) Heat maps depicting differentially expressed genes in *Foxo4*^{*X*^{m+}} versus *Foxo4*^{*X*^{m-}} junctional zones. The heatmap color keys represent z-scores of TPM values. (I) RT-qPCR validation of RNA-seq results ($n=6$ /group). Graphs represent mean \pm s.e.m. Asterisks denote statistical difference (** $P<0.01$; ***) $P<0.001$ as determined by unpaired, two-tailed Student's *t*-test.

replication, extracellular matrix receptor interaction, and complement and coagulation pathways (Fig. 6H; Table S6). Cell cycle and DNA replication signatures may be contributing to the size disparities in wild-type (*Foxo4*^{*X*^{m+}}) versus *Foxo4*^{*X*^{m-}} junctional zone compartments. Junctional adhesion molecule-like (JAML), lipoprotein(a) like 2 (LPAL2), erb-b2 receptor tyrosine kinase 3 (ERBB3), and growth factor receptor bound protein 7 (GRB7) were each conspicuous in their prominent downregulation

(>90% decrease) in FOXO4-deficient junctional zone tissue (Fig. 6I). JAML contributes to epithelial barrier function, modulates immune cell trafficking, and regulates angiogenesis (Kummer and Ebnet, 2018), whereas LPAL2 is a long noncoding RNA contributing to inflammatory and oxidative stress responses (Han et al., 2018). JAML and LPAL2 have not previously been linked to trophoblast or placental biology. ERBB3 is a receptor for neuregulin 1 and promotes trophoblast cell survival

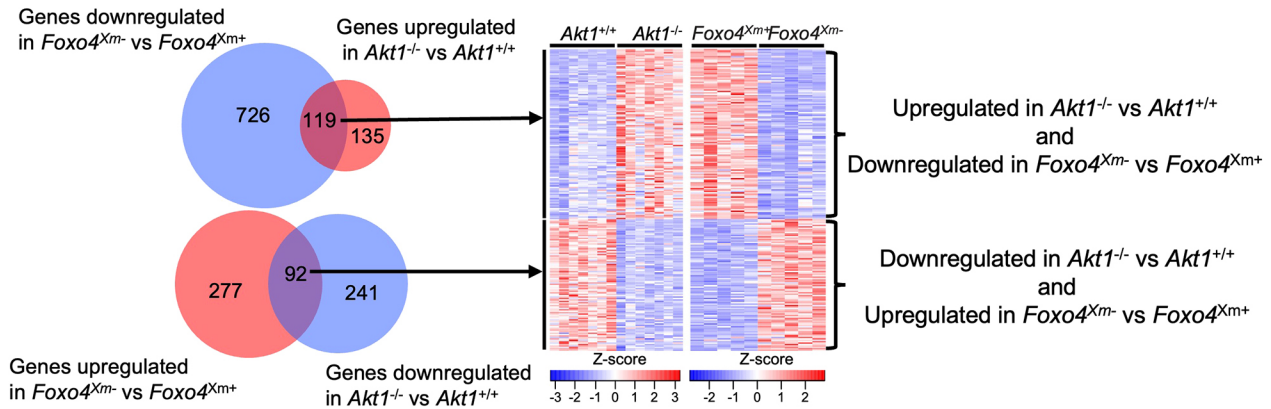


Fig. 7. Reciprocal relationship between AKT1 and FOXO4 in the junctional zone. Venn diagram and heatmaps representing overlap of differentially expressed genes inversely regulated by AKT1 and FOXO4. The heatmap color keys represent z-scores of TPM values.

(Fock et al., 2015) and GRB7 is an adaptor protein participating in signal transduction activated through ERBB3 (Fiddes et al., 1998). Interestingly, numerous junctional zone transcripts regulated by FOXO4 were reciprocally regulated by AKT1 (88% of transcripts upregulated in *Akt1* null were downregulated in *Foxo4* mutant tissues; 38% of transcripts downregulated in *Akt1* null were upregulated in *Foxo4* mutant tissues; Fig. 7). The reciprocal relationship between AKT1 and FOXO4 is evident at structural and molecular levels.

FOXO4 contributes to the regulation of the trophoblast cell lineage

We next modeled junctional zone cell biology using rat TSCs. The consequences of FOXO4 disruption in differentiating rat TSCs were examined. FOXO4 expression was inhibited via ectopic expression of short hairpin RNAs specific to *Foxo4* (Fig. 8A,B). Although a morphologic phenotype was not evident, prominent differences in the transcriptomes of TSCs expressing control versus *Foxo4* shRNAs were observed (Fig. 8C). Disruption of FOXO4 resulted

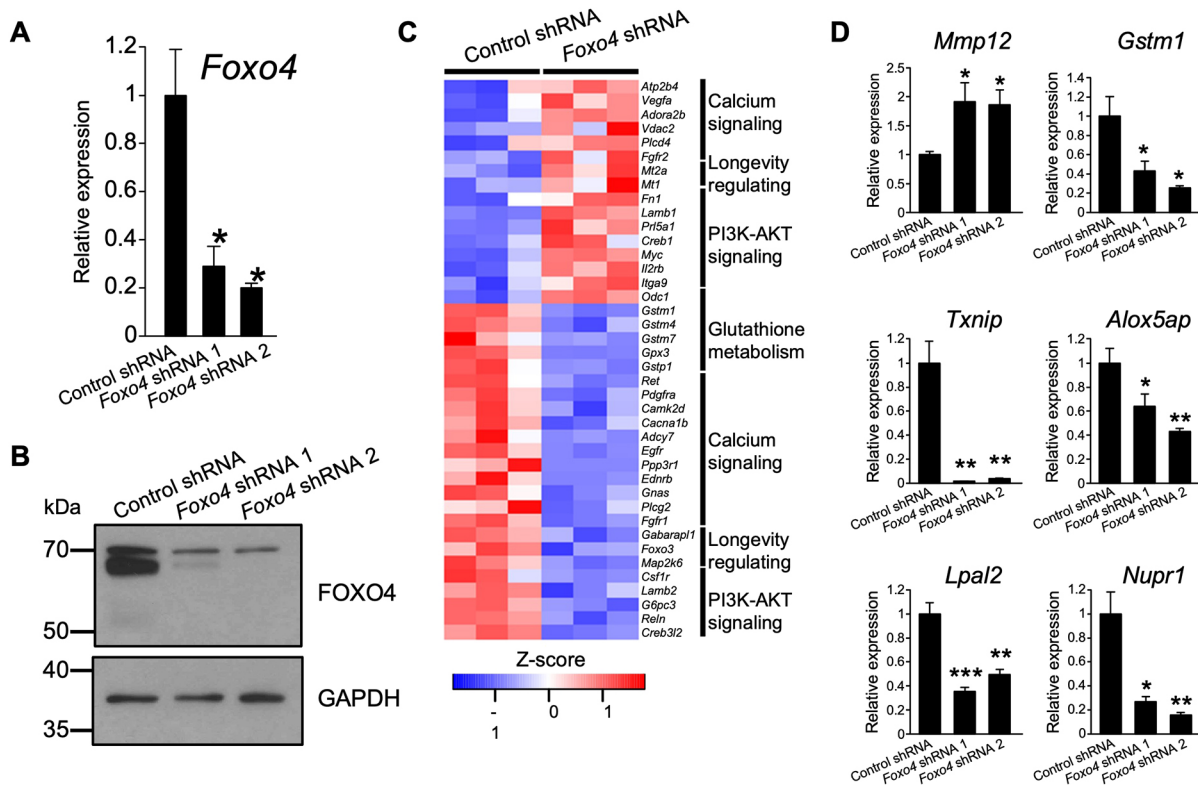


Fig. 8. FOXO4 alters rat TSCs. (A,B) FOXO4 knockdown efficiency was validated by RT-qPCR (A; $n=4$ /group) or western blot (B) analyses in rat TSCs at day 15 of differentiation following transduction with lentivirus containing a control shRNA or one of two independent *Foxo4*-specific shRNAs. Graphs represent mean \pm s.e.m. Asterisks denote statistical difference (versus Control shRNA; * $P<0.05$) as determined by unpaired, two-tailed Welch's *t*-test. (C) Heatmap depicting differentially expressed genes between control and *Foxo4* shRNA-treated rat TSCs. (D) RT-qPCR validation of RNA-seq results (Control shRNA, $n=4$; *Foxo4* shRNA 1, $n=4$; *Foxo4* shRNA 2, $n=4$). Graphs represent mean \pm s.e.m. Asterisks denote statistical difference (compared with Control shRNA; * $P<0.05$; ** $P<0.01$; *** $P<0.001$) as determined by unpaired, two-tailed Welch's *t*-test.

in upregulation of 260 transcripts and downregulation of 443 transcripts (Table S7). Pathway analysis included signatures for PI3K-AKT signaling, longevity regulating, calcium signaling, and glutathione metabolism pathways (Fig. 8C; Table S8). Among the dysregulated transcripts was an upregulation of matrix metalloproteinase 12 (2-fold), a known constituent of endothelial invasive trophoblast cells (Harris et al., 2010; Chakraborty et al., 2016), and downregulation of trophoblast specific protein alpha (3-fold), a transcript characteristic of spongiosotrophoblast cells within the junctional zone (Iwatsuki et al., 2000). FOXO4 is a known regulator of responses to oxidative stress (Liu et al., 2020). Several transcripts associated with inflammatory and cellular stress responses (Sies and Cadenas, 1985; LaFleur et al., 2001; Mashima and Okuyama, 2015; Han et al., 2018; Huang et al., 2021; Nirgude and Choudhary, 2021; Qayyum et al., 2021; Satapathy and Wilson, 2021), including thioredoxin interacting protein (7-fold), glutathione S-transferase mu 1 (3-fold), arachidonate 5-lipoxygenase activating protein (2-fold), interferon kappa (10-fold), nuclear protein 1 (2.7-fold) and *Lpl2* (2.2-fold), were prominently downregulated.

In vivo and *in vitro* disruptions of FOXO4 were consequential, but did not yield identical transcriptomic effects. These discrepancies may reflect intrinsic differences in the cellular compositions of the gd 18.5 junctional zone versus differentiated rat TSCs, *in vivo* versus *in vitro* cell environments, or the null *in vivo* model versus the hypomorphic *in vitro* model.

Key findings

Collectively, the results indicate that AKT1 drives placental growth, including regulation of deep intrauterine trophoblast cell invasion. These actions are accomplished, at least in part, through modulation of FOXO4, which acts to restrain placental growth and coordinate responses to physiological stressors.

DISCUSSION

The rat and human possess a type of hemochorial placentation whereby specialized trophoblast cells penetrate deep into the uterus and transform the uterine parenchyma, including the vasculature (Pijnenborg et al., 1981; Pijnenborg and Vercruysse, 2010; Soares et al., 2012). Central to deep placentation is the source of invasive trophoblast cells, which is a compartment within the placenta referred as the junctional zone in rat and the extravillous trophoblast cell column in human (Soares et al., 2012, 2018; Knöfler et al., 2019). In addition to an intrauterine role, the cellular constituents of these placental compartments produce hormones directed to maternal tissues with actions that ensure *in utero* survival and promotion of fetal growth (Soares et al., 1996; John, 2017). In this study, AKT1 and FOXO4 were identified as regulators of rat junctional zone development. *In vivo* disruption of AKT1 and FOXO4 led to opposite effects on junctional zone development. AKT1 deficiency resulted in growth restriction of the junctional zone, phenotypic alteration of the invasive trophoblast cell lineage, as well as compromised fetal and postnatal growth, and AKT1 was capable of phosphorylating FOXO4 in rat trophoblast cells. Deficiency of FOXO4 resulted in an expanded junctional zone. Deficits in AKT1 or FOXO4 also impacted transcriptomic profiles of the junctional zone. The findings indicate that AKT1 and FOXO4 are part of a gene regulatory network controlling hemochorial placentation.

AKT1 signaling influenced placental development. *Akt1* null mutations in the mouse and rat yield similar phenotypes characterized by placental, fetal and postnatal growth restriction

(Chen et al., 2001; Cho et al., 2001; Yang et al., 2003; Plaks et al., 2011; Kent et al., 2012). Smaller junctional zones accompanying AKT1 deficiency were associated with a downregulation of transcripts encoding proteins driving cell proliferation. These results imply that size differences of junctional zone compartments in the wild type versus *Akt1* nulls were related to, at least in part, diminished trophoblast cell proliferation in *Akt1* junctional zone tissues. The data also fit well with known actions of AKT signaling promoting cell proliferation in a wide range of cell types (Manning and Cantley, 2007; Manning and Toker, 2017; Cole et al., 2019). AKT1 disruption also altered differentiated junctional zone trophoblast cell phenotypes. As cellular constituents of the junctional zone differentiate, they acquire the capacity to express several members of the expanded PRL family of hormones/cytokines (Soares, 2004; Alam et al., 2006; Soares et al., 2007). The expression of PRL8A4, a member of the expanded PRL family, was downregulated in *Akt1* null junctional zones. PRL8A4 is an orphan ligand with little known of its significance to the biology of pregnancy other than as a signature feature of the differentiated junctional zone phenotype (Iwatsuki et al., 1998; Soares et al., 2007). AKT signaling has previously been implicated in the regulation of rodent and human trophoblast cell differentiation (Kamei et al., 2002; Kent et al., 2010, 2011; Haslinger et al., 2013). Disruption of *Akt1* also interfered with invasive trophoblast cell development. Trophoblast cell infiltration into the uterine-placental interface was diminished in *Akt1* nulls. Involvement of AKT signaling has also been implicated in the development of the human extravillous trophoblast cell lineage (Pollheimer and Knöfler, 2005; Haslinger et al., 2013; Morey et al., 2021). AKT signaling could affect invasive trophoblast cell development through its actions on their origin in the junctional zone and extravillous trophoblast cell column or, alternatively, their maturation as they invade into the uterus. Finally, the impact of AKT signaling in invasive trophoblast cell development may be more profound than observed with AKT1 deficiency owing to compensatory activities of AKT2 and AKT3 (Kent et al., 2011; Haslinger et al., 2013).

AKT1 regulates cellular function through its actions as a serine/threonine kinase and, thus, phosphorylation of its substrates (Manning and Cantley, 2007; Manning and Toker, 2017; Cole et al., 2019). The FOX family of transcription factors are well-established targets of AKT action (Lam et al., 2013; Schmitt-Ney, 2020; Herman et al., 2021). Among FOX family members, FOXO4 expression was uniquely elevated in the rat junctional zone. FOXO4 phosphorylation state in trophoblast cells was affected by AKT signaling. AKT-mediated phosphorylation of FOXO4 leads to FOXO4 exit from the nucleus and inactivation (Schmitt-Ney, 2020; Herman et al., 2021), which might suggest that an AKT1 deficiency would result in the stabilization of FOXO4 protein in the junctional zone. Instead, AKT1 deficiency led to depletion of junctional zone total and phosphorylated FOXO4 proteins. Consequently, the observed *Akt1* null placental phenotype was associated with the depletion of both AKT1 and FOXO4 proteins. In addition to regulation by AKT signaling, FOXO4 activity/stability is stimulated by Jun kinase and monoubiquitylation (Essers et al., 2004; van der Horst et al., 2006; Brenkman et al., 2008; Liu et al., 2020), and inhibited by acetylation and polyubiquitylation (Fukuoka et al., 2003; Huang and Tindall, 2011; Liu et al., 2020). Whether AKT1 indirectly affects FOXO4 protein by impacting these other FOXO4 regulators remains to be determined.

FOXO4 is a transcription factor implicated in the regulation of the cell cycle, apoptosis, responses to oxidative stress, and a range of disease processes (Liu et al., 2020). The original characterization of

the *Foxo4* null mouse concluded that FOXO4 did not have a singular role in the pathophysiology of the mouse (Hosaka et al., 2004). The absence of a reported phenotype for the *Foxo4* null mouse model was attributed to the compensatory actions of other members of the FOXO family, including FOXO1, FOXO3, and possibly FOXO6 (Hosaka et al., 2004; Liu et al., 2020). We describe a prominent placental phenotype for the *Foxo4* null rat model. The placental anomalies associated with FOXO4 deficiency were compatible with the production of viable offspring. The absence of a fertility defect in the *Foxo4* null mouse model likely precluded a closer examination of placentation (Hosaka et al., 2004). However, it is also possible that elements of FOXO4 action are species specific. FOXO4 is prominently expressed in the junctional zone and to a lesser extent in invasive trophoblast cells. Disruption of FOXO4 led to an expansion of both junctional and labyrinth zone placental compartments, which probably reflects cell-autonomous and non-cell-autonomous actions, respectively. A striking reciprocal pattern of AKT1 versus FOXO4 gene regulation within the junctional zone was demonstrated and included differentially regulated transcripts encoding proteins involved in the regulation of cell proliferation and cell death. We surmise that AKT1 promotes junctional zone growth by stimulating the expression of transcripts connected to cell cycle progression and inhibiting transcripts connected to cell death, whereas the converse is true for FOXO4. These biological roles are consistent with the known actions of AKT1 and FOXO4 in other cell systems (Manning and Toker, 2017; Liu et al., 2020; Herman et al., 2021). A transcriptional regulatory network involving FOXO4 has also been identified in human extravillous trophoblast cells (Morey et al., 2021). Importantly, FOXO4 also regulates trophoblast cell responses to oxidative stress and is thus positioned to contribute to placental adaptations to a compromised maternal environment and in disease states affecting placentation.

MATERIALS AND METHODS

Animals

Holtzman Sprague-Dawley rats were maintained in an environmentally controlled facility with lights on from 06:00 to 20:00 h with food and water available *ad libitum*. Time-mated pregnancies were established by co-housing adult female rats (8-10 weeks of age) with adult male rats (>10 weeks of age). Detection of sperm or a seminal plug in the vagina was designated gd 0.5. Pseudopregnant females were generated by co-housing adult female rats (8-10 weeks of age) with adult male vasectomized males (>10 weeks of age). The detection of seminal plugs was designated pseudopregnancy day 0.5. Four- to five-week-old donor rats were superovulated by intraperitoneal injection of pregnant mare serum gonadotropin (30 units, G4877, Sigma-Aldrich), followed by an intraperitoneal injection of human chorionic gonadotropin (30 units, C1063, Sigma-Aldrich) ~46 h later, and immediately mated with adult males. Zygotes were flushed from oviducts the next morning (gd 0.5). The University of Kansas Medical Center (KUMC) Animal Care and Use Committee approved all protocols involving the use of rats.

Tissue collection and analysis

Rats were euthanized by CO₂ asphyxiation at designated days of gestation. Uterine segments containing placentation sites were frozen in dry ice-cooled heptane and stored at -80°C until processed for histological analyses. Alternatively, placentation sites were dissected into placentas, the adjacent uterine-placental interface tissue (also referred to as the metrial gland), and fetuses as previously described (Ain et al., 2006). Placentas were weighed and dissected into junctional zone and labyrinth zone compartments (Ain et al., 2006). Placental compartments and uterine-placental interfaces were frozen in liquid nitrogen and stored at -80°C until used for biochemical analyses. Fetuses were weighed, genotyped, and sex determined by PCR (Dhakal and Soares, 2017).

Generation of *Akt1* and *Foxo4* mutant rat models

Mutations at *Akt1* and *Foxo4* loci were generated using CRISPR/Cas9 genome editing (Kaneko, 2017; Iqbal et al., 2021). Guide RNAs targeting exon 4 (target sequence: GCCGTTTGAGTCCATCAGCC; nucleotides 356-375) and exon 7 (target sequence: TTGTCATGGAGTACGCCAAT; nucleotides 712-731) of the *Akt1* gene (NM_033230.3) or targeting exon 2 (target sequence: CCAGATATACGAATGGATGGTCC; nucleotides 517-539) and exon 3 (target sequence: GTTCATCAAGGTACATAACGAGG; nucleotides 631-653) of the *Foxo4* gene (NM_001106943.1) were electroporated into single-cell rat embryos using the NEPA21 electroporator (Nepa Gene Co Ltd). Electroporated embryos were transferred to oviducts of day 0.5 pseudopregnant rats. Initially, offspring were screened for *Akt1* or *Foxo4* mutations from genomic DNA from tail-tip biopsies using the REDExtract-N-Amp™ Tissue PCR kit (XNAT, Millipore Sigma). PCR was performed on the purified DNA samples using primers flanking the guide RNA sites, and products resolved by agarose gel electrophoresis and ethidium bromide staining. Genomic DNA containing potential mutations was amplified by PCR, gel-purified, and precise boundaries of deletions determined by DNA sequencing (Genewiz Inc.). Founders with *Akt1* or *Foxo4* mutations were backcrossed to wild-type rats to demonstrate germline transmission. Routine genotyping was performed by PCR on genomic DNA with specific sets of primers (Table S9).

Western blot analysis

Tissue lysates were prepared using the radioimmunoprecipitation assay lysis buffer system (sc-24948A, Santa Cruz Biotechnology). Protein concentrations were determined using the DC™ Protein Assay Kit (5000112, Bio-Rad Laboratories). Proteins (20 µg/lane) were separated by SDS-PAGE. Separated proteins were electrophoretically transferred to polyvinylidene difluoride membranes (10600023, GE Healthcare) for 1 h at 100 V on ice. Membranes were subsequently blocked with 5% milk or 5% bovine serum albumin for 1 h at room temperature and probed separately with specific primary antibodies to AKT1 (1:1000, 75692, Cell Signaling Technology), pan-AKT (1:1000, 4691, Cell Signaling Technology), phospho-Ser⁴⁷³ AKT (1:2000, 4060, Cell Signaling Technology), FOXO4 (1:2000, 21535-1-AP, Proteintech), phospho-Ser²⁶² FOXO4 (1:3000, ab126594, Abcam), cleaved caspase-3 (Asp175, 1:1000, 9664, Cell Signaling Technology), serine palmitoyltransferase long chain base subunit 3 (LC3B, 1:1000, 2775, Cell Signaling Technology) and glyceraldehyde 3-phosphate dehydrogenase (GAPDH, 1:5000, ab8245, Abcam) in Tris-buffered saline with 0.1% Tween 20 (TBST) overnight at 4°C. After primary antibody incubation, the membranes were washed in TBST three times (10 min each wash) at room temperature. After washing, the membranes were incubated with anti-rabbit or anti-mouse IgG conjugated to horseradish peroxidase [HRP; 1:5000 or 1:20,000 (phospho-Ser²⁶² FOXO4), 7074S and 7076S, Cell Signaling Technology] in TBST for 1 h at room temperature, washed in TBST three times (10 min each wash) at room temperature, immersed in Immobilon Crescendo Western HRP Substrate (WBLUR0500, Sigma-Aldrich), and luminescence detected using Radiomat LS film (Agfa Healthcare) or a Chemi Doc MP Imager (Bio-Rad).

Transcript analysis

Total RNA was extracted from tissues using TRI Reagent Solution (AM9738, Thermo Fisher Scientific) according to the manufacturer's instructions. Total RNA (1 µg) was reverse transcribed using a High-Capacity cDNA Reverse Transcription Kit (4368813, Thermo Fisher Scientific). Complementary DNAs were diluted 1:10 and subjected to reverse transcription-quantitative PCR (RT-qPCR) using PowerUp SYBR Green Master Mix (A25742, Thermo Fisher Scientific) and the primers provided in Table S10. QuantStudio 5 Flex Real-Time PCR System (Applied Biosystems) was used for amplification and fluorescence detection. PCR was performed under the following conditions: 95°C for 10 min, followed by 40 cycles of 95°C for 15 s and 60°C for 1 min. Relative mRNA expression was calculated using the delta-delta Ct method. *Gapdh* was used as a reference transcript.

RNA-seq analysis

Transcript profiles were generated from wild-type and *Akt1*^{-/-}, and *Foxo4*^{loxM} junctional zone tissues, and rat differentiated TSCs expressing control or *Foxo4* shRNAs. Complementary DNA libraries from total RNA samples were prepared using Illumina TruSeq RNA preparation kits according to the manufacturer's instructions (Illumina). RNA integrity was assessed using an Agilent 2100 Bioanalyzer. Barcoded cDNA libraries were multiplexed onto a TruSeq paired-end flow cell and sequenced (100-bp paired-end reads) with a TruSeq 200-cycle SBS kit (Illumina). Samples were run on an Illumina NovaSeq 6000 sequencer at the KUMC Genome Sequencing Facility. Reads from *.fastq files were mapped to the rat reference genome (Ensembl Rnor_5.0.78) using CLC Genomics Workbench 12.0 (QIAGEN). Transcript abundance was expressed as TPM and a *P*-value of 0.05 was used as a cutoff for significant differential expression. Statistical significance was calculated by empirical analysis of digital gene expression followed by Bonferroni's correction. Pathway analysis was performed using Database for Annotation, Visualization, and Integrated Discovery (DAVID; Huang et al., 2009).

Immunohistochemistry

Placentation sites were embedded in optimum cutting temperature (OCT) compound and sectioned at 10 μm thickness using a Leica CM1850 cryostat. Sections were fixed in 4% paraformaldehyde, washed in PBS (pH 7.4) three times (5 min each wash), blocked with 10% normal goat serum (50062Z, Thermo Fisher Scientific), and incubated overnight with primary antibodies: pan cytokeratin (1:300, F3418, Sigma-Aldrich) to identify trophoblast cells; vimentin (1:300, sc-6260, Santa Cruz Biotechnology) to distinguish placental compartments; FOXO4 (1:300, 21535-1-AP, Proteintech); and phospho-Ser²⁶² FOXO4 (1:300, ab126594, Abcam). After washing with PBS (pH 7.4), sections were incubated with corresponding secondary antibodies: Alexa 568-conjugated goat anti-rabbit IgG (1:500, A11011, Thermo Fisher Scientific) or Alexa 568-conjugated rabbit anti-mouse IgG (1:500, A9044, Sigma-Aldrich) for 2 h at room temperature. Sections were then stained with DAPI (1/25,000, D1306, Invitrogen) and mounted using Fluoromount-G mounting media (0100-01, Southern Biotech) and examined microscopically. Fluorescence images were captured on a Nikon 90i upright microscope with a Photometrics CoolSNAP-ES monochrome camera (Roper). The area occupied by cytokeratin-positive cells (invasive trophoblast cells) within the uterine-placental interface was quantified using ImageJ software, as previously described (Nteeba et al., 2020).

In situ hybridization

Distributions of transcripts for *Foxo4* and *Pr17b1* were determined on cryosections of rat placentation sites. RNAScope Multiplex Fluorescent Reagent Kit version 2 (Advanced Cell Diagnostics) was used for *in situ* hybridization analysis. Probes were prepared to detect *Foxo4* (NM_001106943.1, 1038981-C1, target region: 750-1651) and *Pr17b1* (NM_153738.1, 860181-C2, target region: 28-900). Fluorescence images were captured on a Nikon 80i upright microscope with a Photometrics CoolSNAP-ES monochrome camera (Roper).

Rat TSC culture

Blastocyst-derived rat TSCs (Asanoma et al., 2011) were cultured in Rat TS Cell Medium [RPMI 1640 medium (11875093, Thermo Fisher Scientific), 20% (vol/vol) fetal bovine serum (FBS; Thermo Fisher Scientific), 100 μM 2-mercaptoethanol (M7522, Sigma-Aldrich), 1 mM sodium pyruvate (11360-070, Thermo Fisher Scientific), 100 μM penicillin and 50 U/ml streptomycin (15140122, Thermo Fisher Scientific)] supplemented with 70% rat embryonic fibroblast-conditioned medium prepared as described previously (Asanoma et al., 2011), 25 ng/ml fibroblast growth factor 4 (FGF4; 100-31, Peprotech) and 1 μg/ml heparin (H3149, Sigma-Aldrich). For induction of differentiation, rat TSCs were cultured for 15 days in rat TS medium containing 1% (vol/vol) FBS without FGF4, heparin, and rat embryonic fibroblast-conditioned medium. In some experiments, rat TSCs were exposed to a PI3K inhibitor (LY294002, 10 μM, 9901, Cell Signaling Technology), chloroquine (50 μM for 24 h, C6628, Sigma-Aldrich) or staurosporine (1 μM for 3 h, 9953, Cell Signaling Technology) followed by western blot analysis or immunohistochemistry.

Lentivirus construction and production

Lentivirus construction and production were described previously (Muto et al., 2021; Varberg et al., 2021). Briefly, the lentivirus encoding the shRNA targeting *Foxo4* was constructed using a pLKO.1 vector. shRNA oligo sequences used in the analyses are provided in Table S11. Lentiviral packaging vectors were obtained from Addgene and included pMDLg/pRRE (plasmid #12251), pRSV-Rev (plasmid #12253), pMD2.G (plasmid #12259). Lentiviral particles were produced using Attractene (301005, QIAGEN) in human embryonic kidney (HEK) 293FT cells (Thermo Fisher Scientific).

Lentiviral transduction

Rat TSCs were incubated with lentiviral particles for 24 h followed by selection with puromycin dihydrochloride (5 μg/ml; A11138-03, Thermo Fisher Scientific) for 2 days. Cells were then cultured for 1-3 days in Rat TS Cell Medium prior to differentiation.

Statistical analysis

Student's *t*-test, Welch's *t*-test, Dunnett's test or Steel test were performed, where appropriate, to evaluate the significance of the experimental manipulations. Results were deemed statistically significant when *P*<0.05.

Acknowledgements

We thank Stacy Oxley and Brandi Miller for administrative assistance and the KUMC Genome Sequencing Facility for assistance with RNA-seq, including library preparation and sequencing.

Competing interests

The authors declare no competing or financial interests.

Author contributions

Conceptualization: K.K., A.M.-I., M.J.S.; Methodology: A.M.-I., M.-L.W., R.L.S., M.E.S., M.M.; Validation: K.K., A.M.-I., R.L.S., M.E.S., M.M.; Formal analysis: K.K., A.M.-I., K.I., M.J.S.; Investigation: K.K., A.M.-I., K.I., M.-L.W., R.L.S., M.E.S., M.M.; Resources: M.R.P., M.J.S.; Data curation: K.I.; Writing - original draft: K.K., A.M.-I., M.J.S.; Writing - review & editing: K.K., A.M.-I., K.I., M.-L.W., R.L.S., M.E.S., M.M., M.R.P., M.J.S.; Visualization: K.K., A.M.-I.; Supervision: M.J.S.; Project administration: M.J.S.; Funding acquisition: M.J.S.

Funding

This research was supported by postdoctoral fellowships from the Kansas IDeA Network of Biomedical Research Excellence (P20 GM103418 to A.M.-I.), the Lalar Foundation (K.K., A.M.-I., M.M.), the American Heart Association (K.K., M.M.), a National Institutes of Health (NIH) National Research Service Award (HD104495 to R.L.S.) and NIH grants (HD020676, HD079363, HD099638, HD105734), and the Sosland Foundation. Deposited in PMC for release after 12 months.

Data availability

RNA-seq datasets are available at the Gene Expression Omnibus database under accession number GSE205831.

References

- Ain, R., Konno, T., Canham, L. N. and Soares, M. J. (2006). Phenotypic analysis of the rat placenta. *Methods Mol. Med.* **121**, 295-313.
- Alam, S. M., Ain, R., Konno, T., Ho-Chen, J. K. and Soares, M. J. (2006). The rat prolactin gene family locus: species-specific gene family expansion. *Mamm. Genome* **17**, 858-877. doi:10.1007/s00335-006-0010-1
- Aplin, J. D. and Jones, C. J. P. (2021). Cell dynamics in human villous trophoblast. *Hum. Reprod. Update* **27**, 904-922. doi:10.1093/humupd/dmab015
- Asanoma, K., Rumi, M. A., Kent, L. N., Chakraborty, D., Renaud, S. J., Wake, N., Lee, D. S., Kubota, K. and Soares, M. J. (2011). FGF4-dependent stem cells derived from rat blastocysts differentiate along the trophoblast lineage. *Dev. Biol.* **351**, 110-119. doi:10.1016/j.ydbio.2010.12.038
- Asanoma, K., Kubota, K., Chakraborty, D., Renaud, S. J., Wake, N., Fukushima, K., Soares, M. J. and Rumi, M. A. (2012). SATB homeobox proteins regulate trophoblast stem cell renewal and differentiation. *J. Biol. Chem.* **287**, 2257-2268. doi:10.1074/jbc.M111.287128
- Brenkman, A. B., De Keizer, P. L., Van Den Broek, N. J., Jochemsen, A. G. and Burgering, B. M. (2008). Mdm2 induces mono-ubiquitination of FOXO4. *PLoS One* **3**, e2819. doi:10.1371/journal.pone.0002819
- Burton, G. J. and Jauniaux, E. (2018). Pathophysiology of placental-derived fetal growth restriction. *Am. J. Obstet. Gynecol.* **218**, S745-S761. doi:10.1016/j.ajog.2017.11.577

- Burton, G. J., Fowden, A. L. and Thornburg, K. L. (2016). Placental origins of chronic disease. *Physiol. Rev.* **96**, 1509-1565. doi:10.1152/physrev.00029.2015
- Chakraborty, D., Rumi, M. A., Konno, T. and Soares, M. J. (2011). Natural killer cells direct hemochorial placentation by regulating hypoxia-inducible factor dependent trophoblast lineage decisions. *Proc. Natl. Acad. Sci. USA* **108**, 16295-16300. doi:10.1073/pnas.1109478108
- Chakraborty, D., Cui, W., Rosario, G. X., Scott, R. L., Dhakal, P., Renaud, S. J., Tachibana, M., Rumi, M. A., Mason, C. W., Krieg, A. J. et al. (2016). HIF-KDM3A-MMP12 regulatory circuit ensures trophoblast plasticity and placental adaptations to hypoxia. *Proc. Natl. Acad. Sci. USA* **113**, E7212-E7221. doi:10.1073/pnas.1612626113
- Chen, W. S., Xu, P. Z., Gottlob, K., Chen, M. L., Sokol, K., Shiyanova, T., Roninson, I., Weng, W., Suzzuki, R., Tobe, K. et al. (2001). Growth retardation and increased apoptosis in mice with homozygous disruption of the Akt1 gene. *Genes Dev.* **15**, 2203-2208. doi:10.1101/gad.913901
- Cho, H., Thorvaldsen, J. L., Chu, Q., Feng, F. and Birnbaum, M. J. (2001). Akt1/PKBalpha is required for normal growth but dispensable for maintenance of glucose homeostasis in mice. *J. Biol. Chem.* **276**, 38349-38352. doi:10.1074/jbc.C100462200
- Cole, P. A., Chu, N., Salguero, A. L. and Bae, H. (2019). AKTivation mechanisms. *Curr. Opin. Struct. Biol.* **59**, 47-53. doi:10.1016/j.sbi.2019.02.004
- Dash, P. R., Whitley, G. S., Ayling, L. J., Johnstone, A. P. and Cartwright, J. E. (2005). Trophoblast apoptosis is inhibited by hepatocyte growth factor through the Akt and β -catenin mediated up-regulation of inducible nitric oxide synthase. *Cell. Signal.* **17**, 571-580. doi:10.1016/j.cellsig.2004.09.015
- Dhakal, P. and Soares, M. J. (2017). Single-step PCR-based genetic sex determination of rat tissues and cells. *BioTechniques* **62**, 232-233. doi:10.2144/000114548
- Essers, M. A., Weijzen, S., De Vries-Smits, A. M., Saarloos, I., De Ruiter, N. D., Bos, J. L. and Burgering, B. M. (2004). FOXO transcription factor activation by oxidative stress mediated by the small GTPase Ral and JNK. *EMBO J.* **23**, 4802-4812. doi:10.1038/sj.emboj.7600476
- Ferretti, C., Bruni, L., Dangles-Marie, V., Pecking, A. P. and Bellet, D. (2007). Molecular circuits shared by placental and cancer cells, and their implications in the proliferative, invasive and migratory capacities of trophoblasts. *Hum. Reprod. Update* **13**, 121-141. doi:10.1093/humupd/dml048
- Fiddes, R. J., Campbell, D. H., Janes, P. W., Sivertsen, S. P., Sasaki, H., Wallasch, C. and Daly, R. J. (1998). Analysis of Grb7 recruitment by heregulin-activated erbB receptors reveals a novel target selectivity for erbB3. *J. Biol. Chem.* **273**, 7717-7724. doi:10.1074/jbc.273.13.7717
- Fisher, S. J. (2015). Why is placentation abnormal in preeclampsia? *Am. J. Obstet. Gynecol.* **213**, S115-S122. doi:10.1016/j.ajog.2015.08.042
- Fock, V., Plessl, K., Draxler, P., Otti, G. R., Fiala, C., Knöfler, M. and Pollheimer, J. (2015). Neuregulin-1-mediated ErbB2-ErbB3 signalling protects human trophoblasts against apoptosis to preserve differentiation. *J. Cell Sci.* **128**, 4306-4316. doi:10.1242/jcs.176933
- Fukuoka, M., Daitoku, H., Hatta, M., Matsuzaki, H., Umemura, S. and Fukamizu, A. (2003). Negative regulation of forkhead transcription factor AFX (Foxo4) by CBP-induced acetylation. *Int. J. Mol. Med.* **12**, 503-508.
- Gardner, R. L. and Beddington, R. S. (1988). Multi-lineage 'stem' cells in the mammalian embryo. *J. Cell Sci. Suppl.* **10**, 11-27. doi:10.1242/jcs.1988.Supplement_10.2
- Han, B. W., Ye, H., Wei, P. P., He, B., Han, C., Chen, Z. H., Chen, Y. Q. and Wang, W. T. (2018). Global identification and characterization of lncRNAs that control inflammation in malignant cholangiocytes. *BMC Genomics* **19**, 735. doi:10.1186/s12864-018-5133-8
- Harris, L. K., Smith, S. D., Keogh, R. J., Jones, R. L., Baker, P. N., Knöfler, M., Cartwright, J. E., Whitley, G. S. and Aplin, J. D. (2010). Trophoblast- and vascular smooth muscle cell-derived MMP-12 mediates elastolysis during uterine spiral artery remodeling. *Am. J. Pathol.* **177**, 2103-2115. doi:10.2353/ajpath.2010.100182
- Haslinger, P., Haider, S., Sonderegger, S., Otten, J. V., Pollheimer, J., Whitley, G. and Knöfler, M. (2013). Akt isoforms 1 and 3 regulate basal and epidermal growth factor-stimulated SGHPL-5 trophoblast cell migration in humans. *Biol. Reprod.* **88**, 54. doi:10.1095/biolreprod.112.104778
- Hemberger, M. (2002). The role of the X chromosome in mammalian extra embryonic development. *Cytogenet Genome Res.* **99**, 210-217. doi:10.1159/000071595
- Herman, L., Todeschini, A. L. and Veitia, R. A. (2021). Forkhead transcription factors in health and disease. *Trends Genet.* **37**, 460-475. doi:10.1016/j.tig.2020.11.003
- Hosaka, T., Biggs, W. H., 3rd, Tieu, D., Boyer, A. D., Varki, N. M., Cavenee, W. K. and Arden, K. C. (2004). Disruption of forkhead transcription factor (FOXO) family members in mice reveals their functional diversification. *Proc. Natl. Acad. Sci. USA* **101**, 2975-2980. doi:10.1073/pnas.0400093101
- Huang, H. and Tindall, D. J. (2011). Regulation of FOXO protein stability via ubiquitination and proteasome degradation. *Biochim. Biophys. Acta* **1813**, 1961-1964. doi:10.1016/j.bbamer.2011.01.007
- Huang, D., Sherman, B. and Lempicki, R. (2009). Systematic and integrative analysis of large gene lists using DAVID bioinformatics resources. *Nat. Protoc.* **4**, 44-57. doi:10.1038/nprot.2008.211
- Huang, C., Santofimia-Castaño, P. and Iovanna, J. (2021). NUPR1: a critical regulator of the antioxidant system. *Cancers (Basel)* **13**, 3670. doi:10.3390/cancers13153670
- Iqbal, K., Pierce, S. H., Kozai, K., Dhakal, P., Scott, R. L., Roby, K. F., Vyhldal, C. A. and Soares, M. J. (2021). Evaluation of placentation and the role of the aryl hydrocarbon receptor pathway in a rat model of dioxin exposure. *Environ. Health Perspect.* **129**, 117001. doi:10.1289/EHP9256
- Iwatsuki, K., Oda, M., Sun, W., Tanaka, S., Ogawa, T. and Shiota, K. (1998). Molecular cloning and characterization of a new member of the rat placental prolactin (PRL) family, PRL-like protein H. *Endocrinology* **139**, 4976-4983. doi:10.1210/endo.139.12.6373
- Iwatsuki, K., Shinozaki, M., Sun, W., Yagi, S., Tanaka, S. and Shiota, K. (2000). A novel secretory protein produced by rat spongiotrophoblast. *Biol. Reprod.* **62**, 1352-1359. doi:10.1095/biolreprod62.5.1352
- John, R. M. (2017). Imprinted genes and the regulation of placental endocrine function: pregnancy and beyond. *Placenta* **56**, 86-90. doi:10.1016/j.placenta.2017.01.099
- Kamei, T., Jones, S. R., Chapman, B. M., Mcgonigle, K. L., Dai, G. and Soares, M. J. (2002). The phosphatidylinositol 3-kinase/Akt signaling pathway modulates the endocrine differentiation of trophoblast cells. *Mol. Endocrinol.* **16**, 1469-1481. doi:10.1210/mend.16.7.0878
- Kaneko, T. (2017). Genome editing of rat. *Methods Mol. Biol.* **1630**, 101-108. doi:10.1007/978-1-4939-7128-2_9
- Kent, L. N., Konno, T. and Soares, M. J. (2010). Phosphatidylinositol 3 kinase modulation of trophoblast cell differentiation. *BMC Dev. Biol.* **10**, 97. doi:10.1186/1471-213X-10-97
- Kent, L. N., Rumi, M. A., Kubota, K., Lee, D. S. and Soares, M. J. (2011). FOSL1 is integral to establishing the maternal-fetal interface. *Mol. Cell. Biol.* **31**, 4801-4813. doi:10.1128/MCB.05780-11
- Kent, L. N., Ohboshi, S. and Soares, M. J. (2012). Akt1 and insulin-like growth factor 2 (Igf2) regulate placentation and fetal/postnatal development. *Int. J. Dev. Biol.* **56**, 255-261. doi:10.1387/ijdb.1134071k
- Knipp, G. T., Audus, K. L. and Soares, M. J. (1999). Nutrient transport across the placenta. *Adv. Drug Deliv. Rev.* **38**, 41-58. doi:10.1016/S0169-409X(99)00005-8
- Knöfler, M., Haider, S., Saleh, L., Pollheimer, J., Gamage, T. K. J. B. and James, J. (2019). Human placenta and trophoblast development: key molecular mechanisms and model systems. *Cell. Mol. Life Sci.* **76**, 3479-3496. doi:10.1007/s00018-019-03104-6
- Kubota, K., Kent, L. N., Rumi, M. A., Roby, K. F. and Soares, M. J. (2015). Dynamic regulation of AP-1 transcriptional complexes directs trophoblast differentiation. *Mol. Cell. Biol.* **35**, 3163-3177. doi:10.1128/MCB.00118-15
- Kummer, D. and Ebnét, K. (2018). Junctional adhesion molecules (JAMs): the JAM-integrin connection. *Cells* **7**, 25. doi:10.3390/cells7040025
- Lafeur, D. W., Nardelli, B., Tsareva, T., Mather, D., Feng, P., Semenuk, M., Taylor, K., Buerigin, M., Chinchilla, D., Roshke, V. et al. (2001). Interferon-kappa, a novel type I interferon expressed in human keratinocytes. *J. Biol. Chem.* **276**, 39765-39771. doi:10.1074/jbc.M102502200
- Lam, E. W., Brosens, J. J., Gomes, A. R. and Koo, C. Y. (2013). Forkhead box proteins: tuning forks for transcriptional harmony. *Nat. Rev. Cancer* **13**, 482-495. doi:10.1038/nrc3539
- Liu, W., Li, Y. and Luo, B. (2020). Current perspective on the regulation of FOXO4 and its role in disease progression. *Cell. Mol. Life Sci.* **77**, 651-663. doi:10.1007/s00018-019-03297-w
- Maltepe, E. and Fisher, S. J. (2015). Placenta: the forgotten organ. *Annu. Rev. Cell Dev. Biol.* **31**, 523-552. doi:10.1146/annurev-cellbio-100814-125620
- Manning, B. D. and Cantley, L. C. (2007). AKT/PKB signaling: navigating downstream. *Cell* **129**, 1261-1274. doi:10.1016/j.cell.2007.06.009
- Manning, B. D. and Toker, A. (2017). AKT/PKB signaling: navigating the network. *Cell* **169**, 381-405. doi:10.1016/j.cell.2017.04.001
- Mashima, R. and Okuyama, T. (2015). The role of lipoxygenases in pathophysiology; new insights and future perspectives. *Redox Biol.* **6**, 297-310. doi:10.1016/j.redox.2015.08.006
- Morey, R., Farah, O., Kallol, S., Requena, D. F., Meads, M., Moretto-Zita, M., Soncin, F., Laurent, L. C. and Parast, M. M. (2021). Transcriptional drivers of differentiation, maturation, and polyploidy in human extravillous trophoblast. *Front. Cell Dev. Biol.* **9**, 702046. doi:10.3389/fcell.2021.702046
- Muto, M., Chakraborty, D., Varberg, K. M., Moreno-Irusta, A., Iqbal, K., Scott, R. L., McNally, R. P., Choudhury, R. H., Aplin, J. D., Okae, H. et al. (2021). Intersection of regulatory pathways controlling hemostasis and hemochorial placentation. *Proc. Natl. Acad. Sci. USA* **118**, e2111267118. doi:10.1073/pnas.2111267118
- Nirgude, S. and Choudhary, B. (2021). Insights into the role of GPX3, a highly efficient plasma antioxidant, in cancer. *Biochem. Pharmacol.* **184**, 114365. doi:10.1016/j.bcp.2020.114365
- Nteba, J., Varberg, K. M., Scott, R. L., Simon, M. E., Iqbal, K. and Soares, M. J. (2020). Poorly controlled diabetes mellitus alters placental structure, efficiency, and plasticity. *BMJ Open Diabetes Res. Care* **8**, e001243. doi:10.1136/bmjdr-2020-001243

- Pijnenborg, R. and Vercruyse, L.** (2010). Animal models of deep trophoblast invasion. In *Placental Bed Disorders* (ed. R. Pijnenborg, I. Brosens and R. Romero), pp. 127-139. Cambridge: Cambridge University Press.
- Pijnenborg, R., Robertson, W. B., Brosens, I. and Dixon, G.** (1981). Trophoblast invasion and the establishment of haemochorial placentation in man and laboratory animals. *Placenta* **2**, 71-91. doi:10.1016/S0143-4004(81)80042-2
- Plaks, V., Berkovitz, E., Vandoorne, K., Berkutzki, T., Damari, G. M., Haffner, R., Dekel, N., Hemmings, B. A., Neeman, M. and Harmelin, A.** (2011). Survival and size are differentially regulated by placental and fetal PKBalpha/AKT1 in mice. *Biol. Reprod.* **84**, 537-545. doi:10.1095/biolreprod.110.085951
- Pollheimer, J. and Knöfler, M.** (2005). Signalling pathways regulating the invasive differentiation of human trophoblasts: a review. *Placenta* **26**, S21-S30. doi:10.1016/j.placenta.2004.11.013
- Qayyum, N., Haseeb, M., Kim, M. S. and Choi, S.** (2021). Role of thioredoxin-interacting protein in diseases and its therapeutic outlook. *Int. J. Mol. Sci.* **22**, 2754. doi:10.3390/ijms22052754
- Qiu, Q., Yang, M., Tsang, B. K. and Gruslin, A.** (2004). Both mitogen-activated protein kinase and phosphatidylinositol 3-kinase signalling are required in epidermal growth factor-induced human trophoblast migration. *Mol. Hum. Reprod.* **10**, 677-684. doi:10.1093/molehr/gah088
- Roberts, R. M., Green, J. A. and Schulz, L. C.** (2016). The evolution of the placenta. *Reproduction* **152**, R179-R189. doi:10.1530/REP-16-0325
- Satpathy, S. and Wilson, M. R.** (2021). The dual roles of clusterin in extracellular and intracellular proteostasis. *Trends Biochem. Sci.* **46**, 652-660. doi:10.1016/j.tibs.2021.01.005
- Schmitt-Ney, M.** (2020). The FOXO's advantages of being a family: considerations on function and evolution. *Cells* **9**, 787. doi:10.3390/cells9030787
- Sharma, N., Kubaczka, C., Kaiser, S., Nettersheim, D., Mughal, S. S., Riesenberger, S., Hölzel, M., Winterhager, E. and Schorle, H.** (2016). Tpbpa-Cre-mediated deletion of TFAP2C leads to deregulation of Cdkn1a, Akt1 and the ERK pathway, causing placental growth arrest. *Development* **143**, 787-798. doi:10.1242/dev.128553
- Shukla, V. and Soares, M. J.** (2022). Modeling trophoblast cell-guided uterine spiral artery transformation in the rat. *Int. J. Mol. Sci.* **23**, 2947. doi:10.3390/ijms23062947
- Sies, H. and Cadenas, E.** (1985). Oxidative stress: damage to intact cells and organs. *Philos. Trans. R. Soc. Lond. B Biol. Sci.* **311**, 617-631. doi:10.1098/rstb.1985.0168
- Soares, M. J.** (2004). The prolactin and growth hormone families: pregnancy-specific hormones/cytokines at the maternal-fetal interface. *Reprod. Biol. Endocrinol.* **2**, 51. doi:10.1186/1477-7827-2-51
- Soares, M. J., Chapman, B. M., Rasmussen, C. A., Dai, G., Kamei, T. and Orwig, K. E.** (1996). Differentiation of trophoblast endocrine cells. *Placenta* **17**, 277-289. doi:10.1016/S0143-4004(96)90051-X
- Soares, M. J., Konno, T. and Alam, S. M.** (2007). The prolactin family: effectors of pregnancy-dependent adaptations. *Trends Endocrinol. Metab.* **18**, 114-121. doi:10.1016/j.tem.2007.02.005
- Soares, M. J., Chakraborty, D., Rumi, M. A. K., Konno, T. and Renaud, S. J.** (2012). Rat placentation: an experimental model for investigating the hemochorial maternal-fetal interface. *Placenta* **33**, 233-243. doi:10.1016/j.placenta.2011.11.026
- Soares, M. J., Varberg, K. M. and Iqbal, K.** (2018). Hemochorial placentation: development, function, and adaptations. *Biol. Reprod.* **99**, 196-211. doi:10.1093/biolre/iqy049
- Takagi, N. and Sasaki, M.** (1975). Preferential inactivation of the paternally derived X chromosome in the extraembryonic membranes of the mouse. *Nature* **256**, 640-642. doi:10.1038/256640a0
- Van Der Horst, A., De Vries-Smits, A. M., Brenkman, A. B., Van Triest, M. H., Van Den Broek, N., Colland, F., Maurice, M. M. and Burgering, B. M.** (2006). FOXO4 transcriptional activity is regulated by monoubiquitination and USP7/HAUSP. *Nat. Cell Biol.* **8**, 1064-1073. doi:10.1038/ncb1469
- Varberg, K. M., Iqbal, K., Muto, M., Simon, M. E., Scott, R. L., Kozai, K., Choudhury, R. H., Aplin, J. D., Biswell, R., Gibson, M. et al.** (2021). ASCL2 reciprocally controls key trophoblast lineage decisions during hemochorial placenta development. *Proc. Natl. Acad. Sci. USA* **118**, e2016517118. doi:10.1073/pnas.2016517118
- West, J. D., Papaioannou, V. E., Frels, W. I. and Chapman, V. M.** (1978). Preferential expression of the maternally derived X chromosome in extraembryonic tissues of the mouse. *Basic Life Sci.* **12**, 361-377. doi:10.1007/978-1-4684-3390-6_25
- Wooding, P. and Burton, G.** (2008). *Comparative Placentation*. Heidelberg, Germany: Springer-Verlag.
- Yang, Z. Z., Tschopp, O., Hemmings-Mieszczak, M., Feng, J., Brodbeck, D., Perentes, E. and Hemmings, B. A.** (2003). Protein kinase B alpha/Akt1 regulates placental development and fetal growth. *J. Biol. Chem.* **278**, 32124-32131. doi:10.1074/jbc.M302847200

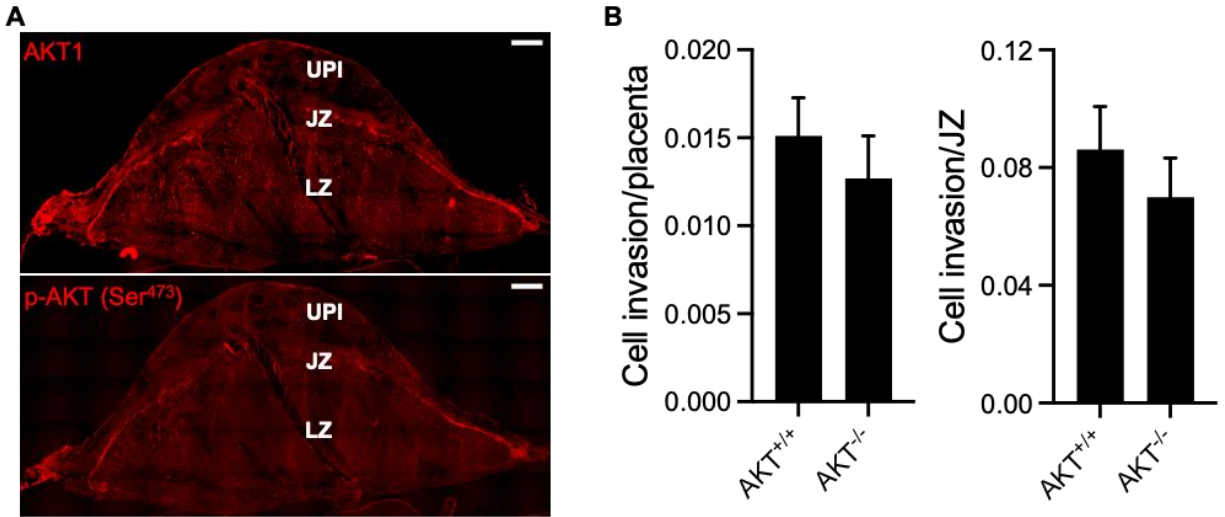


Fig. S1. Placental AKT protein distribution and intrauterine trophoblast cell invasion in wild type and *Akt1* null placentation sites. **A)** Distribution of AKT1 (top) and phospho (p)-AKT4 (Ser⁴⁷³) proteins (bottom) in the gestation day (**gd**) 18.5 placentation site. **B)** Area occupied by invasive trophoblast cells (cytokeratin-positive cells) within the uterine-placental interface was quantified and is presented relative to areas associated with the entire placenta or the junctional zone (**JZ**). Graphs represent means ± SEM (n = 6/group).

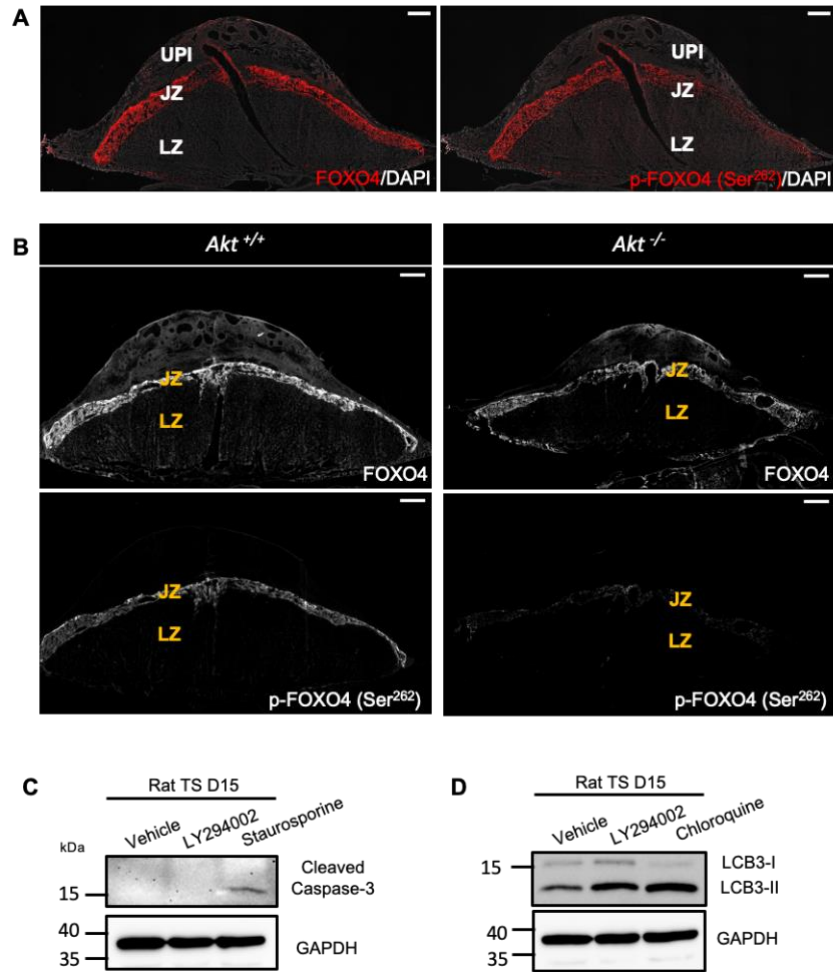


Fig. S2. Relationship of PI3K/AKT signaling to FOXO4 distribution and functions. A) Distributions of FOXO4 and phospho (p)-FOXO4 (Ser²⁶²) proteins in gestation day (gd) placentation sites. **B)** Distribution of FOXO4 and phospho (p)-FOXO4 (Ser²⁶²) proteins in *Akt*^{+/+} and *Akt*^{-/-} placentas at gd 18.5. UPI: uterine-placental interface; JZ: junctional zone; and LZ: labyrinth zone. **C)** Western blot analysis of cleaved caspase-3 in rat TS cells exposed to vehicle (DMSO), LY294002 (10 μ M), or staurosporine (1 μ M). Staurosporine was used as a positive control. **D)** Western blot analysis for serine palmitoyltransferase long chain base subunit 3 (LCB3) in rat TS cells exposed to vehicle (DMSO), LY294002 (10 μ M), or chloroquine (50 μ M). Chloroquine was used as a positive control. Please note that inhibition of PI3K/AKT signaling did not have a detectable effect on the formation of cleaved caspase-3 but did have a modest effect on LCB3 accumulation.

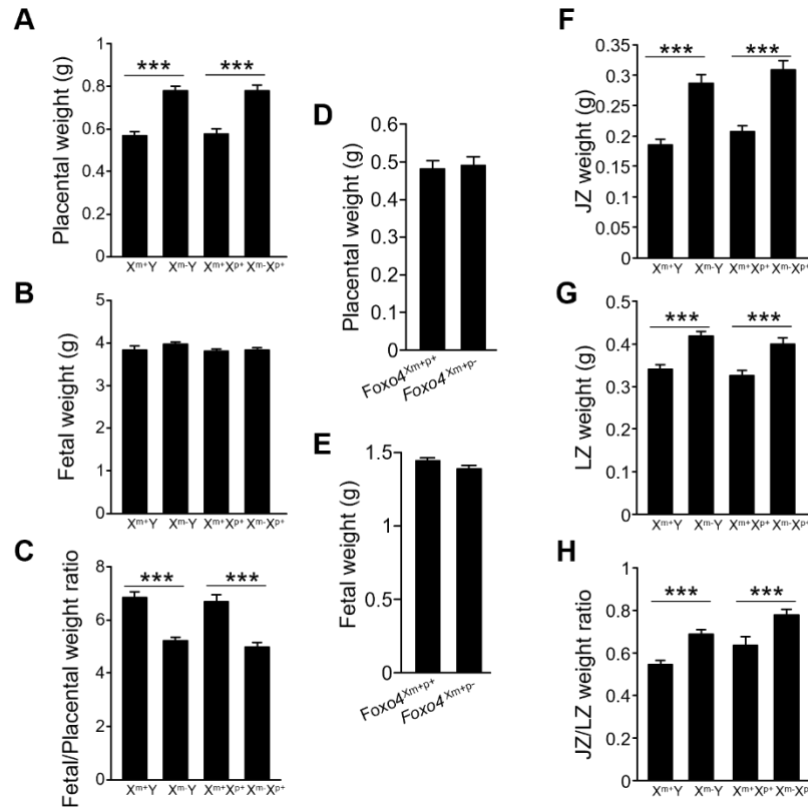


Fig. S3. Placentas (**A**) and fetuses (**B**) were dissected from *Foxo4* heterozygous females mated with wild type males at gd 20.5 and weighed; **C**, fetus/placenta ratio. Placentas (**D**) and fetuses (**E**) were dissected from wild type females mated with *Foxo4* hemizygous null males at gd 18.5 and weighed. **F-H**) Placentas from heterozygous females mated with wild type males were then separated into junctional zone (**JZ**, **F**) and labyrinth zone (**LZ**, **G**) compartments, and weighed; **H**, JZ/LZ weight ratio. $X^{m+}Y$, $n = 19$; $X^{m-}Y$, $n = 22$; $X^{m+}X^{p+}$, $n = 15$; $X^{m-}X^{p+}$, $n = 15$ from 6 dams. Graphs represent means \pm SEM. Asterisks denote statistical differences (***) $P < 0.001$ as determined by Student's or Welch's *t*-test.

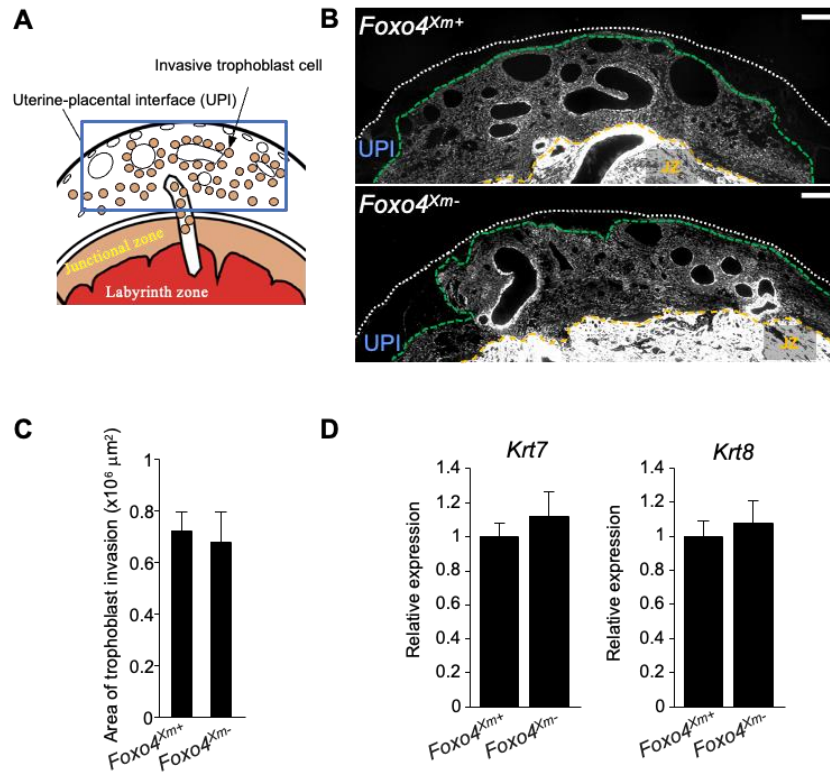


Fig. S4. FOXO4 deficiency does not affect either intrauterine trophoblast invasion or the intrauterine invasive trophoblast cell phenotype. **A)** Schematic representation of a late gestation placentation site. The uterine-placental interface, site for intrauterine trophoblast invasion, is highlighted in the boxed area. **B)** Trophoblast cells were immunostained for pan-cytokeratin (**KRT**). Representative images are shown. The extent of intrauterine trophoblast invasion is demarcated using a green dashed line. The white dotted line represents the outer border of the uterus, and the yellow dashed line represents the uterine border with the placenta. Scale bars = 500 μm . **C)** The area of intrauterine trophoblast invasion is graphically depicted ($n = 6/\text{group}$). Graphs represent means \pm SEM. **D)** RT-qPCR measurements of *Krt7* and *Krt8* transcripts, signature markers for invasive trophoblast cells, within dissected uterine-placental interface tissue specimens at gd 18.5 (*Foxo4^{Xm+}*, $n = 12$; *Foxo4^{Xm-}*, $n = 12$). Graphs represent means \pm SEM.

Table S1. Genotype of offspring following *Akt1* heterozygous breeding.

| Offspring from <i>Akt1</i> ^{+/-} x <i>Akt1</i> ^{+/-} | Offspring genotype | | |
|---|----------------------------|----------------------------|----------------------------|
| | <i>Akt1</i> ^{+/+} | <i>Akt1</i> ^{+/-} | <i>Akt1</i> ^{-/-} |
| Total | 40 | 92 | 42 |
| Ratio (%) | 23 | 52.9 | 24.1 |

Table S2. RNAseq AKT1 WT vs KO JZ

[Click here to download Table S2](#)

Table S3. AKT KO JZ Pathway analysis

[Click here to download Table S3](#)

Table S4. Genotype of offspring following *Foxo4* hemizygous male x wild type female breeding.

| Offspring from X⁻Y x XX | Offspring genotype | |
|--|------------------------|-------------------------------------|
| | X^{m+}Y | X^{m+}X^{p-} |
| Total | 40 | 44 |
| Ratio (%) | 47.6 | 52.4 |

Table S5. RNAseq Foxo4 WT vs KO JZ

[Click here to download Table S5](#)

Table S6. Foxo4 KO JZ Pathway analysis

[Click here to download Table S6](#)

Table S7. RNAseq Foxo4 KD in rTSC

[Click here to download Table S7](#)

Table S8. Foxo4 KD rTS Pathway analysis

[Click here to download Table S8](#)

Table S9. Primers used for genotyping

| Primer name | Sequence |
|-------------------|--------------------------|
| <i>Akt1</i> Fwd | TGAGTCCATTCTGGAGGACTAGAC |
| <i>Akt1</i> Rev1 | TTGCCAGTAGCTTCAGGTACTION |
| <i>Akt1</i> Rev2 | GAGGGAAGGTTAGGGACTAGCC |
| <i>Foxo4</i> Fwd | AGAAGGTACCCACGGAGGGA |
| <i>Foxo4</i> Rev1 | CCACACAGTTCCTGCTGTACATAG |
| <i>Foxo4</i> Rev2 | CTCCTTGGAGTGGCACCTTC |

Fwd, forward

Rev, reverse

Table S10. List of primers used for RT-qPCR

| Gene | Forward primer | Reverse primer | Accession no. | Amplicon size (bp) |
|----------------|---------------------------|---------------------------|----------------|--------------------|
| <i>Ccn3</i> | CATGGTTCGGCCTTGTGAG | TGGATTTACAGGACTTCTTGGT | NM_030868.2 | 89 |
| <i>Cend1</i> | AATGCCAGAGGCGGATGAGA | CGTTGTGCGGTAGCAGGAGA | NM_171992.5 | 190 |
| <i>Ccne1</i> | TGCAGGCGAGGATGAGA | GAAGTCCTGTGCCAAGTAGAATG | NM_001100821.1 | 98 |
| <i>Cdc6</i> | CAGGCGAGCTATTGAAATTGTG | GACTTGGGATATGTGAGCGAGA | NM_001108298.1 | 130 |
| <i>Cdk1</i> | GTTGACATCTGGAGCATAGG | CTCTACTTCTGGCCCACTT | NM_019296.2 | 144 |
| <i>Mcm5</i> | TGTCAGGATTTACCAAACA | CACTTGAGGCGGTAAGCAC | NM_001399204.1 | 123 |
| <i>Prl8a4</i> | CTGAAACCCTCTGTAATCTTGCTG | GTCTCGTCCCTCTAATCAGTTTG | NM_021580.1 | 112 |
| <i>Krt7</i> | CGGAATGGAACCTGTGAA | GTAGATGTAGTCTTGATGGAATAAG | NM_001047870.2 | 150 |
| <i>Krt8</i> | TGGGCCAGGAGAAGCTGAA | CACATCCTTGATGAGGACAAA | NM_199370.1 | 140 |
| <i>Foxo4</i> | CGGAATGCCTGGGGAAA | ATGTACCTTGATGAACCTGCTGTG | NM_001106943.1 | 213 |
| <i>Grb7</i> | TACCACCTGGAGAGAAGAGAGAGAG | GGGCTCAGATCCAGTTCCA | NM_053403.2 | 141 |
| <i>ErbB3</i> | TGCGTTGCCAGTTGTCC | CCGTGCTTATCTACTCCATCTTGT | NM_017218.3 | 92 |
| <i>JamL</i> | TCGGCCTTGATGGGATG | CACGCTGAGGCTGGAGTAGTAG | XM_032909807.1 | 129 |
| <i>Lpal2</i> | AAGGAGATGCCAACCAACAAA | GCCATTCTCCCTCCTGA | NM_001109578.1 | 125 |
| <i>Mmp12</i> | GCTGGTTCGGTTGTTAGG | GTAGTTACACCCTGAGCATAC | NM_053963.2 | 100 |
| <i>Gstm1</i> | CTGGACGCCTTCCAAA | TAGCAAGGGCCTACTTGTACTCC | NM_017014.2 | 145 |
| <i>Txnip</i> | GTCTCAGCAGTGCAAACAGACC | AAGCTCAAAGCCGAACCTGTACTC | NM_001008767.2 | 139 |
| <i>Alox5ap</i> | TGTGGGCAATGTTGTGCTC | GCTTTGCGCCTTGCTTC | NM_017260.2 | 100 |
| <i>Nupr1</i> | GCCCACTTCCAGCA | ACCTCCACCGACGACATAAGA | NM_053611.2 | 102 |
| <i>Gapdh</i> | GACATGCCGCCTGGAGAAAC | AGCCCAGGATGCCCTTAGT | NM_017008.4 | 92 |

Table S11. shRNA sequences

| shRNA | Sequence |
|----------------------|---|
| <i>Foxo4</i> shRNA 1 | CCGGTGCAGTCCTTGTCTCGAAACTCGAGTTTCGAGGACAAGGACTGCTTTTTG |
| <i>Foxo4</i> shRNA 2 | CCGGTGCTTGCATCTCCTACTGAACTCGAGTTCAGTAGGAGATGCAAGCTTTTTG |